

# Design Practice and Operational Experience of Highly Irradiated, High Performance Normal Magnets

Joel H. Schultz<sup>1</sup>

*Received March 15, 1983*

---

The fundamental limitations, design practice, and operating experience of high-stress and highly irradiated normal magnets are discussed. Magnet performance is limited by mechanical stresses, temperature limits, oxidation, and erosion. Electrical performance is limited by dielectric breakdown, flashover, and tracking. Degradation of mechanical and electrical properties of metals and insulators by electromagnetic and neutron irradiation is discussed. The failure mechanisms due to irradiation include increased conductor resistance, destruction of chemical bonds, electrolysis, and photoconductivity. The operating experience of high-performance magnets at magnet laboratories, accelerators, and fusion experimental facilities is discussed.

---

**KEY WORDS:** magnet; high field magnet; irradiated magnet; copper magnet.

## 1. INTRODUCTION

The title of this paper is a misnomer, as there are no magnets which can really be considered to be simultaneously high performance (high mechanical stress, high current density, high electric field, high coolant velocity) and highly irradiated (by neutrons, gamma rays, or X-rays). However, the well-established trends of the two most important users of large air core magnets, the thermonuclear fusion and particle physics programs, strongly suggest the need for such magnets in future reactors and accelerators. In both programs, there is a high order dependence of all physics figures of merit on magnetic field and a first order dependence of cost on magnet aperture. Since magnet aperture can only be decreased by decreasing physics performance or by decreasing the radiation shielding of the magnets, there is a need to develop high performance, lightly shielded magnets.

Although the ultimate goal of a highly irradiated, high performance solenoid magnet has not been

achieved, a number of magnets that are either high performance or highly irradiated have been designed, built and operated. Many high performance magnets have been built for the purpose of investigating the effects of high magnetic fields in matter, most notably at solid-state physics laboratories, such as the M.I.T. Francis Bitter National Magnet Laboratory. Magnets in which one or another allowable parameter has been highly stressed exist throughout the fusion, particle physics, magnetohydrodynamics, and solid state physics programs. Irradiated magnets have, so far, been used exclusively in particle physics, but have been designed for the first major neutron producing experiments in magnetic confinement: the Tokamak Fusion Test Reactor (TFTR) at Princeton and the Joint European Tokamak (JET) at Culham, England. A review of the design practice and operating experience of these magnets is a logical starting point for the design of more ambitious future generation magnets. Unfortunately, there has never been a development program specifically aimed at characterizing either high performance or highly irradiated magnets. Almost all of the magnets that have

<sup>1</sup>Plasma Fusion Center, M.I.T., Cambridge, Massachusetts.

been built support scientific programs considered to be more important than the magnets themselves, so that the magnet histories are poorly recorded. The irradiation of magnets in accelerators is generally not measured. Erosion rates of material in high performance magnets are not measured. Electric fields and mechanical stresses in magnets are frequently not measured.

## 2. LIMITATIONS OF HIGH PERFORMANCE MAGNETS

### 2.1. Mechanical Limits

Like all structures, magnets are limited by the strength of the materials used in the magnet. All magnets must have a conductor, usually copper and occasionally aluminum. Most magnets have an insulation system and a structural case or internal structural reinforcement, usually of stainless steel. Magnets are usually considered to be a type of pressure vessel by their designers, because of the similarity of the force fields created in a magnet winding by magnetic field and those created in a containment vessel by pressurized fluids. Recently, large magnets have been designed according to the specifications of the ASME Pressure Vessel Code [AS80]. A tabulation of the specifications in the Power Boiler Code for Nuclear Power Plant Components is shown in Table I. The three large copper magnet systems for TFTR, JET, and JT-60 are built to similar overall design allowable limits, as shown in Table II.<sup>(13,60,81,93)</sup> The peak stress intensities in copper vary between 170 and 220 MPa (25–32 ksi).

Operating experience at the National Magnet Laboratory suggests a recommended design peak stress of 25 ksi in copper, according to R. Weggel (FBNML, private communication, 1980). The stress in the insulation has generally been dominated by the clamping prestress at about a level of 2 ksi. Most of the designs Weggel worked on were coils with uniaxial tensile stresses. While the most common failure mode has been insulator aging, particularly in Kapton insulation, which has low resistance to aging by water, there have been occasional failures caused by yielding in the copper, leading to explosion of the magnet. This is at a design stress level of 25 ksi, overall. These may be considered fatigue failures, in that they don't occur on the magnet's first shot at full current.

Table I. ASME Boiler Code Limitations on Material Stress

Primary yield	2/3
Ultimate tensile strength	1/3
Membrane plus bending	min(YS, 1/2 UTS)
Primary buckling	0.2

Table II. Design Allowables in Large Normal Magnets

Parameter	TFTR	JET	JT-60	Units
Copper tensile stress		90		(MPa)
Copper compressive stress		80		(MPa)
Copper stress intensity			220	(MPa)
Copper temperature	65.5	72		(C)
Structure stress intensity			380	(MPa)
Insulation compressive stress				(MPa)
Insulation shear stress		5		(MPa)
Water temperature				(C)
Water velocity				(m/s)
Peak current density (Overall conductor)		2.7	2.68	(kA/cm <sup>2</sup> )
Peak voltage	2.0	4.6	7.5	(kV)
Layer-layer voltage		288		(V)
Turn-turn voltage	9	12		(V)

In an irradiated environment, H. Becker (M.I.T. Plasma Fusion Center, private comm.) has designed to a stress in G-10 of 18 ksi, using thin disks or sheets of insulation, no greater than 20 mils thick. For fatigue-limited operation, Becker recommended a design stress of 20 ksi for either an epoxy or polyimide composite matrix. The reason that they are both the same is that, after irradiation, most of the strength is coming from the glass filler.

#### 2.1.1. Availability and Size Limitations

Surveys that have been made at the National Magnet Laboratory indicated the following capabilities of domestic manufacturers, as of 1981. Revere can cold roll copper to widths of 120 in., in thicknesses up to 10 in., and in lengths over 20 ft. G. O. Carlsen can hot roll steel to widths of 196 in. According to Becker (private comm.), Revere rolls copper in 5 foot widths to thicknesses between  $\frac{1}{2}$  in. and 2 in., routinely. The faces of the composite sheets in Zephyr were to be cemented with epoxy to the copper and steel plates adjacent to it. Two 48 in. widths of G-10 sheet were to be cemented together to form the insulation for the Zephyr TF coils.

## 2.2. Temperature Limits

Magnet temperatures and heat generation are limited by aging of the insulation, annealing of copper, and boiling of liquid coolants, such as water. Temperature limits are also linked to stress limits through the thermal stresses generated by temperature differences within a magnet.

### 2.2.1. Temperature Limits of Copper

Copper temperatures are limited by annealing of cold-worked copper, oxidation of copper, and thermal stresses, usually due to interturn temperature differentials. According to manufacturer's curves from Amax, 200 C is a temperature at which cold-worked copper begins to anneal. The application literature of Pyrotenax of Canada, Ltd., suggests that 250 C is the temperature limit of copper if one wishes to avoid progressive oxidation. A table of the decrease of copper sheath thickness versus time and temperature shows a loss of 1 mil in 2.57 years at 250 C, 2 mils in 10.3 years at 250 C, 1 mil in 0.0583 years at 400 C, and 2 mils in 0.233 years at 400 C.

### 2.2.2. Temperature Limits of Insulation

Organic insulations are temperature limited due to depolymerization reactions and outgassing of water. The absorption of water and the chemical attack of water on copper-insulation bonds, in axially cooled magnets are also accelerated by increased temperature. A typical manufacturers' recommended design limit for epoxies is 65–85 C. Polyimides are preferred at elevated temperatures, up to 250–300 C. R. Weggel (private comm.) of the M.I.T. National Magnet Laboratory recommended a temperature limitation of 100 C for polyimide insulations immersed in water and 150 C for insulations that are protected from water, in order to avoid aging of the insulator. Magnets at FBNML have been run to 150 C, immersed in water, and have failed. The most common failure mode is embrittlement of the insulation, cracking of the insulation, and some form of dielectric breakdown through the water gap.

*Aging: Insulation Endurance Limits.* Organic polymers can be destroyed by reverse depolymerization reactions, accelerated by the presence of electric

field and elevated temperature. In the case of temperature alone, the aging rate has the form of the Arrhenius equation:

$$R_t = Ae^{B/T}$$

where  $A$  and  $B$  are characteristic constants of the material. The most popular model of the endurance of insulation against voltage is the inverse power law<sup>(96)</sup>:

$$L_e = cG^{-n}$$

where  $L_e$  is the electrical life,  $G$  is the electrical stress, and  $c$  and  $n$  are constants.

There are various ways to combine these models, which are not necessarily compatible, in an integrated model of insulator aging. A key to an integrated model is the observation that insulator lifetime tends to infinity below a certain value of voltage gradient  $G_S$ ,<sup>(96)</sup> called the threshold gradient. Dakin first proposed a model using a threshold gradient<sup>(28)</sup> that was in good agreement with experimental data, although it is inconsistent with the Arrhenius model:

$$L_e = \alpha \frac{\exp(-h/G)}{G - G_S}$$

where  $\alpha$  and  $h$  are material constants at the frequency of interest, and  $G$  is the electrical field. In tests done by Simoni<sup>(96)</sup> on a polyaliphatic epoxy and on a layer of Mylar between two layers of Nomex, the threshold field for the epoxy resin was 0.15 of the short-time breakdown field, while the threshold for the Mylar-Nomex sandwich was 0.17–0.19 of the short-time breakdown field. The existence of a threshold temperature is also inferred from the unified aging theory of Simoni, related to the threshold voltage by

$$\frac{G_B}{G_{s0}} - 1 = \frac{1}{(T_{s0}/T_o) - 1}$$

so that for an insulator with a  $G_{s0}$  between 0.17 and 0.19,  $T_{s0}$  varies between 77 and 86 C.

*Insulation Water Loss.* A special concern for insulations in a vacuum environment is that outgassing of water at elevated temperatures could cause significant weight loss and degradation of mechanical properties. The insulation testing program for the Tokamak Fusion Test Reactor (TFTR) tested high temperature effects on several candidate vacuum

chamber insulations,<sup>(84)</sup> including the polyimide based Vespel SP-1 (DuPont), PMR-15 (Grumman), and Kapton Type-H (DuPont), along with two inorganic bonded micas. The insulator materials were aged at elevated temperatures in the inert gas argon. At 350 C, Kapton Type-H lost 6% of its weight in 65 h, and PMR-15 lost 3% of its weight in 120 h. After an initial dip in weight of 1% in Vespel SP-1, probably due to water vapor outgassing, the weight remained stable at 350 C to 120 h. Outgassing caused a pressure buildup in a mass spectrometer of greater than  $5 \times 10^{-6}$  torr at 400 C for PMR-15 and at 500 C for Vespel SP-1. This pressure buildup was not reached for either of the micas, up to 1000 C. Changes in postaging mechanical properties could not be unambiguously detected.

### 2.2.3. Cooling Limitations

Magnet cooling is limited by the surface heat flux into the water that can be supported without boiling and by the need to remove heat from the inside to the outside of a magnet, which is particularly a problem for internally cooled conductors. Heat removal also ties into the abovementioned limitations in thermal stresses, as well as the temperature limitations, which are the primary purpose of cooling systems. The maximum heat flux from copper to water has been studied in the most depth by manufacturers of evacuated tubes, for applications such as the anodes, vanes, and cavities of radio frequency transmitters,<sup>(68)</sup> and, more recently, by the magnetic fusion program for neutral-beam injector grids<sup>(50)</sup> and neutral beam dump calorimeters.<sup>(46, 47)</sup> These programs have provided the benchmarks for the ultimate performance of copper-water cooling systems. The 15 A, 120 keV, 0.5 s pulse facility at the Lawrence Berkeley Laboratory is designed to a maximum heat flux density of 2.6 kW/cm<sup>2</sup> for 0.5 s, with a projected heat flux on the acutely angled cooling surface of 20.5 kW/cm<sup>2</sup>.<sup>(46)</sup>

The National Magnet Laboratory routinely runs steady-state Bitter magnets at current densities up to 10,000–15,000 A/cm<sup>2</sup>. Coolant holes are about 2 mm diameter and spacings are about 2 mm. The water velocity is typically 15 m/s. The average lifetime of these magnets is 100–150 h, with insulation failure dominating. The copper hot-spot design temperature is 150 C. R. Weggel (private comm.) recommends designing to a calculated heat flux of 500 W/cm<sup>2</sup> for a “reliable” magnet. FBNML operates water-cooled

magnets routinely at heat fluxes of 1000–1500 W/cm<sup>2</sup>. Typical water velocities are 10 m/s and a typical Reynold's number is 10,000. P. Griffith (M.I.T., private comm.) suggests that two practical rules-of-thumb for high performance water cooling systems are to keep the temperature of the water at least 100 F below saturation at the design pressure at all points in the cooling loop and to build a full-scale model of the system, burn it out, and design to half the burn-out heat flux.

According to S. Thomson (Bechtel, private comm.), standard industrial practice in large utilities is to restrict the inlet water for a cooling system to no lower than 105 F. Typical velocities in the plumbing from the pump buildings to the reactor cell is 15 m/s. Pumps can be expected to be at least 80% efficient. There should be about a nominal head loss of 100 feet in the main. If the calculated head loss is greater than 100 feet, a separate water line should be used. The load water outlet temperature should be limited to less than 200 C or 100 C in an unpressurized system.

*Oxidation.* Oxidation of copper surfaces is suspected of being an occasional cause of magnet failure. It is mentioned in manufacturer's literature as being the cause of temperature limits (see Section 2.2.1), implying that it is more restrictive than copper annealing. Oxidation at mechanical contacts, leading to hot spots, accelerated oxidation, and ultimately burnout, is certainly a cause of magnet failure. Copper oxide whiskers have been found in water-cooled magnets built at the National Magnet Laboratory (see below), but are not known to be a cause of failure. The oxidation of copper in air has been reviewed by Rönquist<sup>(86)</sup> and others.

Oxidation rate laws are usually presented as approximate solutions in limiting cases of a general rate equation, first proposed by Mott<sup>(74)</sup>:

$$\frac{dy}{dt} = C \sinh \frac{E}{ykT}$$

where  $y$  is the thickness of the oxide layer, and  $E$  is the energy of activation for the migration of cations in the direction of growth under the influence of concentration and electrical potential gradients. Over limited ranges of thickness and temperature, diffusion based rate laws can be approximated by a relation of the form:

$$m^n = Kt$$

where, in the magnet range of temperatures,  $n$  is generally found to equal 2. In other words, the thickness of the coating increases with the square root of time. However, according to Campbell and Thomas,<sup>(18)</sup> the oxide formation rate at 100 C is  $0.06t^{1/3}$  ( $\mu\text{g}/\text{cm}^2$ ), where  $t$  is the time (s).

*Erosion.* Dielectric breakdown in water is usually not a problem, since the high dielectric constant of water, as well as its ability to carry away ions in solution, give it a high dielectric strength, typically 500 kV/cm.<sup>(11)</sup> However, the presence of chemically active species in aqueous solution as well as the hydraulic forces exerted by a high performance water cooling system can lead to rapid erosion and failure of a copper/insulator magnet structure. Erosion of copper by cooling water is observed when the impurity level of the water is too high (or, paradoxically, too low) or when the velocity of the water is sufficiently high that the dynamic head of the coolant becomes a few percent of the yield strength of copper. A lower limit for erosion of copper by deionized water was measured by Johnson<sup>(57)</sup> in standing water at 38 C. The initial rate of weight change was  $0.025 \mu\text{g}/\text{cm}^2\text{-day}$  at 38 C, with a saturation value of  $0.14 \mu\text{g}/\text{cm}^2$  with a water concentration of 1.2 mg/L. Saturation is due to the formation of a protective copper oxide coating.

Erosion of copper tubing by water under various conditions was studied by Knutsson,<sup>(62)</sup> using tap water from the Finspang Water Works. The temperature, pH, oxygen content, water velocity, and tubing size were varied, and the tubes were inspected after 12 months. The most significant result was the beneficial effect of deaeration. Deaerated water with a pH of 8.0 could be run up to 12.0 m/s with no observable depth of attack. Aerated water with a pH of 8 could only be run to 3 m/s with no observable corrosion at 65 C and 6.0 m/s at 30 C. If the aerated water had a pH of 6.5, corrosive attack was found when the velocity was  $>1$  m/s. No differences in corrosion resistance were observed between annealed and hard-drawn copper tubes, even at the highest water velocities.

Corrosion of a large number of structural materials by pure water (resistivity  $>1 \times 10^6 \Omega\text{-cm}$ ) was studied by Roebuck et al. at Argonne.<sup>(85)</sup> Copper was screened against a number of materials, including stainless steel, which had the highest corrosion resistance, and was rated in the low corrosion resistance group, along with bronze and plain carbon

steels. Unfortunately, the exact quantitative results are not reported. However, it can be inferred from this report that somewhere between 300 and 400 F, the erosion rate of copper is  $0.3 \text{ mg}/\text{cm}^2\text{-mho}$  at a water velocity of 30 ft/s. Since this is a very high erosion rate, corresponding to 3.4 mm/year, it implies that the water temperature should be kept below 300 F.

The erosion of different alloys of copper was measured by Von H. Sick,<sup>(92)</sup> using water at velocities of 4.7, 8, and 12 m/s. The best performance was by CuNi30Fe, which eroded at a rate of 0.1 mm/year in 12 m/s water and 0.03 mm/year in 4.7 m/s water. The worst performance at 12 m/s was by CuNi5Fe, which eroded at 0.26 mm/year, while the worst performance at 4.7 m/s was by CuZn30, which eroded at 0.09 mm/year. Thus there was about a factor of three difference between the best and worst alloy at each water velocity. The water had a pH of 7.5 with impurities including 7 mg/L of oxygen, 16 mg/L of chloride, 27 mg/L of sulfates, and 35 mg/L of silicic acid.

Marshakov<sup>(70)</sup> has established a relation between the erosion rate and the resistivity of the water. Copper corroded uniformly in all the water samples he studied at a rate of  $0.0041\text{--}0.0065 \text{ mg}/\text{cm}^2\text{-day}$ . The depletion of oxygen in the water drops the rate of copper corrosion to  $0.0004 \text{ mg}/\text{cm}^2\text{-day}$ . The corrosion rate of both copper and brass is found to be minimum in water with a specific resistance of 1  $\text{M}\Omega\text{-cm}$ . Tunder<sup>(97)</sup> compared the corrosion currents of copper into water of different compositions, in the range of 2–10  $\text{M}\Omega\text{-cm}$ . Using sodium sulfate, copper sulfate, sodium carbonate, and ferrous sulfate solutions, Tunder concluded that the effect of an additive cannot be predicted solely in terms of its effect on conductivity, pH, or any other general aqueous property. Erosion of copper by high speed water has been observed at the National Magnet Laboratory, but has not led to any known magnet failures. Water is distilled and deionized, before being run through the magnets, to a purity of  $10^6 \Omega\text{-cm}$ .<sup>(99)</sup> Weggel (private comm.) infers the existence of erosion from the presence of a powdery black residue in the water and a coating of CuO on all the copper surfaces in contact with cooling water (see below).

No magnet failures are attributed to erosion at mechanical joints. However, pitting has been observed at joints. In one case, when a magnet was inspected, it was found that the Belleville washers providing the "follow-up" of the bolted contact were

rattling and that a large part of the first turn had been eaten away. One of the high-field magnets at the S.N.C.I. facility in Grenoble, France (see below) had joints with hydraulic clamping, to avoid the loss of clamping pressure through bolt loosening.

*Water Resistivity.* It is widely recognized that the conductivity of water in a water-cooled magnet must be held to a relatively low value. The quantitative effects of water conductivity on erosion and corrosion are discussed further below, including radiolytic effects. The effect of water conductivity on leakage currents is always a design concern in axially cooled magnets, but is too obvious to require discussion here. This section reviews design practice in the selection of water resistivity. The magnet shop of the Princeton Plasma Physics Laboratory (K. Wakefield, private comm., 1982) used chilled deionized water in the PDX and PLT tokamaks with a design level of water conductivity of  $0.2 \mu\text{S}/\text{cm}$  and an alarm-trip level of about  $0.5 \mu\text{S}/\text{cm}$ . Measured values of conductivity in these cooling circuits is typically  $0.12\text{--}0.17 \mu\text{S}/\text{cm}$ , but a few unusual instances have been recorded during which operations continued when the resistivity was about a factor of 10 lower than normal (K. Wakefield, private comm.). At FBNML (M. J. Leupold, private comm.), a fraction of initially distilled water is bled through a deionizing and a demineralizing bed in order to keep magnet cooling water at a conductivity of  $1 \mu\text{S}/\text{cm}$ . The water resistivity is monitored, but there are no trip levels.

## 2.3. Electrical Limits

### 2.3.1. Dielectric Breakdown in Air

The dielectric strength of air is described by the familiar Paschen's law:

$$V = f(pd)$$

which has a voltage minimum of 300 V at a pressure-distance product of  $pd = 5 \text{ mmHg}\cdot\text{cm}$ . Gaps of more than  $10^{-2} \text{ cm}$  in air at s.t.p. have density-distance values far higher than that at the minimum Paschen voltage, and the breakdown voltage increases monotonically with  $pd$ . In air, the formula for the breakdown voltage is<sup>(15)</sup>:

$$V = 24.22 \frac{293p}{700T} d + 6.08 \sqrt{\frac{293p}{760T} d}$$

where  $p$  is the pressure (mmHg),  $T$  is the temperature (K),  $d$  is the gap (cm), and  $V$  is the voltage (kV). In a uniform field, the dielectric strength (kV/cm) is

$$E = 24.22 + \frac{6.08}{\sqrt{d}}$$

which has an asymptotic value of 24 kV/cm at long gaps.

*Corona.* According to Alston,<sup>(4)</sup> if the maximum stress in a gap is less than five times the mean stress, breakdown phenomena are very similar to those in a uniform field. At higher stress ratios, corona ionization may be maintained locally in the region of high stress. Peek<sup>(78)</sup> obtained relations for corona inception field in air between cylinders. For concentric cylinders, with an inner cylinder radius  $r$  (cm), the corona inception field (kV/cm) is

$$E_i = 31p \left( 1 + \frac{0.308}{\sqrt{pr}} \right)$$

where  $p$  is the air pressure (atm). The corona inception field for parallel cylinders with radius  $r$  (cm) is nearly identical:

$$E_i = 30p \left( 1 + \frac{0.301}{\sqrt{pr}} \right)$$

### 2.3.2. Dielectric Breakdown in Helium

Although this paper deals exclusively with the failure mechanisms of normal magnets, dielectric breakdown in helium is included here, both because normal magnets can be gas cooled and because the mechanisms of failure are similar in all gases, helium being one of the best studied. The dielectric strength of liquid helium is comparable to that of air at standard temperature and pressure. Unfortunately, since breakdown accompanies heating due to a normal event and rapidly heats local helium, the actual breakdown strength of liquid helium in a magnet is hard to interpret. It is conservative and probably correct to always consider gaseous helium to be the insulant in a pool boiling magnet.

The breakdown strength of gaseous helium at ambient temperature is only a small fraction of that of air because the electrons can gather kinetic energy

from electrical field drift up to the ionization level in this noble gas. Paschen's law should hold for gaseous helium at any temperature. The Paschen curve shows that no breakdown can occur in helium below 160 V, corresponding to a density-spacing product value of  $1 \times 10^5$  (kg/m<sup>3</sup>)-m, or a gap of less than 1  $\mu$ m filled with helium vapor at 4.2 K. However, as soon as the helium density exceeds 15–20 kg/m<sup>3</sup>, the Paschen law is no longer valid and field emission becomes dominant. D. Marcowitz, a senior magnet designer at Intermagnetics General, reports that the PMS coil for TRW was built with an insulator flashover design field of 20 V/mil across the insulating spacer (private comm.). Marcowitz has built a magnet that flashed over at 30–40 V/mil. The design method for the PMS coil was to take the Paschen curve worst pressure breakdown field at 300 K and then add a safety factor.

Johnson et al.<sup>(58)</sup> measured a large number of ground insulation samples that simulated the insulation system for the toroidal and poloidal field coils of the Princeton Tokamak Fusion Test Reactor (TFTR). A 100 mil kapton-glass epoxy and a 375 mil epoxy-glass ground wrap were tested. A relatively high statistical spread was observed between the best and worst specimens in a test, about a factor of 2 for low cycle ac tests. For high cycle survival at 60 Hz, it is necessary to design to 100 V/mil (37.5 kV) with the epoxy-glass. There were fewer cycles with kapton-glass epoxy, but it appears that 500 V/mil (50 kV) is necessary to be below the minimum voltage to failure. However, corona was detected across 100 mil insulation at 3.8 kV (38 V/mil) for the fiberglass-epoxy insulation and at 6.8 kV (68 kV) for the kapton-glass epoxy insulation.

May and Krauth studied the influence of electrode surface conditions on the breakdown of liquid helium at 1 atm.<sup>(71)</sup> Over a range of 0.5–3.0 mm gaps, the breakdown voltage of electropolished niobium, the best surface, varied from 25 kV (50 kV/mm) to 92 kV at 2 mm (46 kV/mm), while the breakdown voltage of brass, the worst surface, varied from 8 kV at 0.5 mm (16 kV/mm) to 40 kV at 3.0 mm (13 kV/mm). The breakdown was a strong function of time, interpreted as the growth of a channel of superheated helium with a very slow rate of heat removal (characteristic time of 5 h). Hwang and Hong<sup>(56)</sup> measured dielectric breakdown in liquid and gaseous helium across epoxy insulation and arrived at flashover fields of 24 kV/mm in liquid helium at 0.27 mm and 12 kV/mm (400 V/mil) in gaseous helium.

This degraded slightly at the higher gap length of 0.63 mm to 18 kV/mm in liquid helium and 10.5 kV/mm (250 V/mil) in gaseous helium at 4.2 K. The point-to-plane dielectric strength of epoxy at 4.2 K was 136 kV/mm (3000 V/mil). The point-to-plane dielectric strength of helium is at least 2.5 kV/mm (60 V/mil) up to a separation gap of 2 mm.

Olivier<sup>(77)</sup> measured voltage breakdown in helium as a function of conditioning and electrode polarity. He discovered a large conditioning effect and occasional deconditioning. A 0.5 mm gap in liquid helium between brass and steel had an initial breakdown voltage of 25 kV on the first discharge, a minimum breakdown voltage of 12 kV on the 24th discharge, and a maximum breakdown voltage of 55 kV on the last and 50th discharge. The vast majority of breakdowns occurred with the brass electrode as the cathode. However, the ratios of the maximum and minimum breakdown voltages are not highly dependent on the electrode polarity. Thoris et al.<sup>(96)</sup> investigated striking distances between electrodes in helium over a range of temperatures and at high voltages. They discovered a  $1/T$  dependence of the breakdown voltage over a broad range of temperatures. They also found dramatic deterioration of the breakdown electric field at large gaps. This is particularly striking at high voltages. For instance, within the limitations of a very large graph-reading error, a peak voltage of 10 kV requires a gap of 6 mm at 30 K (40 V/mil), 17 mm at 60 K (15 V/mil), and 80 mm at 240 K (3 V/mil).

D. Weldon (LASL, CTR-9, private comm., 1980) has designed and tested many high-voltage leads, up to a lead to ground voltage of 60 kV, pulsed over 2 ms. These leads have  $\frac{1}{4}$  in. G-10 sleeves, which were fit directly over the leads. One of these leads has failed; it burned up, accompanied by high thermal stresses and cracking of the insulation, leading to arcover through the crack. The lead insulation has a nominal dielectric strength of over 1000 V/mil. Weldon stated that helium should generally be designed to have a dielectric strength 5–10 times worse than air. In air, one might design to a striking field of 25 V/mil and a tracking field of 5–10 V/mil. Weldon's numbers come from Haarman and Williamson,<sup>(45)</sup> who also reported nearly identical tracking breakdown fields for paper phenolic, polyethylene, nylon, and teflon. Therefore, the tracking strength for any wrap should be about 4 kV/cm. A factor of 5 safety margin would imply that tracking should be limited to 2 V/mil. Typical electrical de-

sign limits in a cryogenic environment are:

Flashover along an insulating spacer in helium	7 V/mil
Tracking along an insulating wrap	2 V/mil
Breakdown through an epoxy	150 V/mil
Breakdown through a kapton wrap	1000 V/mil
Maximum temperature on quench	120 K

### 2.3.3. Flashover and Dielectric Breakdown in Vacuum

Flashover is loosely defined as dielectric breakdown along the surface of an insulator. It is distinguished from tracking by its sudden avalanchelike character and is distinguished from arcing by the dominance of surface effects. The dielectric strength of the surface of an insulator is always weaker than that of a vacuum gap of similar dimensions. The strength of high voltage standoffs for utility applications is made to be greater than that of air by crenellating the insulator surface in order to make the flashover length much greater than the air gap between electrodes. In a magnet, substantial enhancement of the path length along an insulator is frequently not possible. Therefore, unless one can design a magnet with clever, crenellated standoffs between layers, the problems of flashover and dielectric breakdown in vacuum are essentially identical.

Flashover is believed to be caused by secondary electron emission leading to positive charging of the insulator surface. The necessary condition for initiating a breakdown event is that the applied electric field exceed a threshold value at the cathode vacuum/conductor/insulator junction, permitting field emission of electrons. Positive charging of the insulator can occur when the secondary electron emission ratio is greater than 1. For most insulations, this regime begins at a primary electron lower energy level of 20–100 eV and ends at a higher energy level of 1–5 keV. The positive charging of the insulation leads to enhancement of the electric field at the cathode/insulator interface. The positively charged insulator reattracts the secondary electrons, so an avalanche of electrons can “hop” along the insulator surface from the cathode to the anode. The buildup of charge can be extremely rapid, typically tens of nanoseconds, while the relaxation of charge is slow in

vacuum, typically several hours at a pressure of  $10^{-9}$  torr.<sup>(16)</sup> The dominant relaxation mechanism is believed to be the bulk electronic relaxation time of the insulating material, so that the time is not expected to decrease linearly with pressure.

A dominant feature of flashover in vacuum is the role of gas that is desorbed thermally or electronically from the insulator surface. This gas is assumed to create an ionizable medium in the vicinity of the surface that can support the regenerative ionization processes that permit arcing. Anderson<sup>(5)</sup> showed that low thermal conductivity insulators could develop a temperature rise adequate for rapid desorption of gas in a few nanoseconds. Ohki<sup>(76)</sup> found indirect experimental evidence that the surface flashover voltage of polyethylene decreases with temperature according to a model of surface gas desorption. More recently, Anderson and Brainard<sup>(6)</sup> developed a theoretical model based on electron stimulated desorption of gas, which showed good agreement between experimental observations and the predicted dependence of the breakdown delay time on the length of the insulator and electric field. Cross<sup>(27)</sup> suggests a similar model which assumes that the secondary electron emission avalanche is followed by a final flashover stage, initiated by a large burst of electron emission from the cathode insulator junction. This burst charges successive regions of the insulator negatively until the burst reaches the anode, leaving a channel of excited gas in its wake along which flashover occurs. A few procedures, relevant to magnet design, can be used to improve the resistance to flashover of an insulating spacer.

1. *Junction shaping*: The shape of the insulator, in particular, its angle with the metal electrodes, can be used to control the trajectories of the secondary electrons, improving the flashover voltage. A bibliography of junction shaping approaches is included in Latham.<sup>(66)</sup>

2. *Magnetic insulation*: As with vacuum gap breakdown, a transverse magnetic field will also suppress insulation flashover, as shown by Bergeron and McDaniel.<sup>(11)</sup> If the magnetic field is transverse to the electric field, as would normally be expected between the layers of a solenoid magnet, there is a critical impedance ratio  $R_c$  between the impedance of the load and the region in the vicinity of the insulator, above which an avalanche will be depleted:

3. *Material selection*: According to Latham,<sup>(66)</sup> there is a considerable divergence among the pub-



lished data as to the correct hierarchy of materials versus surface flashover. However, there is a consensus that the best insulators have a glasslike structure, because of the superior resistance to gas evolution in comparison with porous ceramics or organic insulations.

4. *Surface roughening*: Gleichauf<sup>(41)</sup> found that roughening of the insulator near the cathode interface improved flashover performance.

5. *Surface coating*: If a material were found with a secondary electron emission yield less than one for all impact energies, flashover presumably could not occur. Insulating materials generally have high values of secondary electron emission, while metals and semiconductors are low. Good results have been obtained using  $\text{Fe}_2\text{O}_3$ <sup>(36)</sup> and  $\text{Cr}_2\text{O}_3$ <sup>(94)</sup> coatings. DC insulating performance can be improved by a factor of 2–3 using coatings, while surge protection is less marked. It is almost impossible to create a secondary electron emission yield which is less than one for all impact energies, because of the yield enhancement that occurs at glancing angles of incidence, which are common in avalanche.

All methods of voltage flashover are very sensitive to surface contamination. Chatterton and Davies<sup>(23)</sup> have systematically studied the effect of contamination of the hold-off voltages of Macor, Lucalox, and Plexiglas insulators. They were able to form a model of flashover conditioning, showing improvement of hold-off voltage after successive flashovers for uncoated surfaces. However, they were unable to form such a model for the more complex case of insulators coated with C or Ti, which is believed to be a better simulation of surface conditions after flashover.

#### 2.3.4. Tracking

Tracking is the leakage current due to the formation of a conducting path across the surface of an insulator. In most cases, the conduction results from degradation of the insulation itself, implying organic insulation. However, in the case of the water-cooled inorganic insulations postulated for highly irradiated magnets, tracking may also be observable. The conducting film is usually moisture from the atmosphere absorbed by some form of contamination, such as dust. Tracking does not depend upon Paschen breakdown and can occur at well below 100 V in air, while a gaseous discharge at s.t.p. cannot exist below

380 V. Degradation of the insulation is caused by heat from tracking, which either carbonizes or volatilizes the insulation. Carbonization results in a permanent extension of the electrodes and usually takes the form of a dendritic growth. Erosion of the insulation also occurs, although the dominant failure mechanism is usually carbonization.

Low-voltage test methods for tracking have been established by the International Electrotechnical Commission (I.E.C.) in *Publication 112*. Two chisel-edged electrodes, usually of brass, are rested on a horizontal test piece 4 mm apart. Drops of a specified size of 0.1% ammonium chloride solution fall between the electrodes at 30 s intervals. A curve of drops-to-failure versus voltage is then constructed. At a particular voltage, called the comparative tracking index (CTI), this curve becomes asymptotic. CTI values on the I.E.C. test range from 100 to 140 for a phenolic bonded paper board, to 200 to 300 for mineral-filled alkyd resins, to 600 for silicone rubber. Many of the materials with the highest CTI's would fail by erosion.<sup>(30)</sup>

### 3. MAGNET LIMITS UNDER IRRADIATION

Magnets that are highly irradiated by neutrons, gamma rays, or X-rays have the same limitations as unirradiated magnets, as well as some entirely new limitations. The limitations on irradiated magnets can be placed in three broad categories: (a) fluence-related changes in bulk material properties, (b) flux-related acceleration or catalysis of surface electrochemistry, and (c) new chemistry and new structural behavior due to the creation of otherwise absent species or microstructures. Almost all of the study of radiation limits on materials has concentrated on the first category. Almost all magnet failures, one suspects, will be caused by the latter two.

#### 3.1. Properties of Candidate Insulations for a Highly Irradiated Environment

##### 3.1.1. Irradiated Properties of G-10

G-10, a fiberglass reinforced epoxy, is the most popular insulation for large, air-core magnets in both the cryogenic and room-temperature environments for nonirradiated magnets. G-10 has also been selected for the mildly irradiated toroidal field mag-

nets of TFTR. Recent experiments conducted on the INEL reactor by Erez and Becker<sup>(32)</sup> confirmed Becker's theory that G-10 in thin disks will have considerably higher strength after irradiation than G-10 rods. The total dose was  $10^{11}$  rads of gamma radiation,  $10^{19}$  (n/cm<sup>2</sup>) at energies greater than 0.1 MeV and  $10^{20}$  total (n/cm<sup>2</sup>). Twenty mil disks of G-10 withstood 200 MPa (30 ksi) peak stress under cyclic loading at room temperature for 200,000 cycles without any observable failure. Some samples also withstood up to 85,000 cycles at 207 MPa (40 ksi) peak stress. G-7 samples failed at 30 ksi after 10,000 cycles. G-11 samples with a thickness of 150 mils showed partial destruction after 10,000 cycles. Promising inorganic insulations are discussed in the next several sections, but a recent experiment by Erez and Becker<sup>(32)</sup> is a strong counterindicator for mica-glass, the most popular inorganic sheet insulation. Simulating the insulation conditions for Zephyr, a German ignition experiment using cryocooled Bitter plates, 0.5 mm samples of G-7, G-10, and mica-glass were tested for unirradiated compression fatigue. While a stack of 5 G-10 specimens, separated by steel plates, survived 60,000 cycles at a maximum applied stress of 310 MPa (45 ksi), several mica-glass samples failed at 10,000 cycles at 207 MPa (30 ksi). G-10 was irradiated to a level of  $1.6 \times 10^{19}$  n/cm<sup>2</sup> for neutron energies greater than 0.1 Mev,  $10^{20}$  n/cm<sup>2</sup> for all neutrons and  $3.8 \times 10^{11}$  rads of gamma radiation, simulating an environment similar to that planned for the resistive toroidal field magnets in Zephyr.<sup>(102)</sup> A stack of 5 irradiated G-10 samples survived 200,000 cycles at a peak compressional stress of 207 MPa (30 ksi). Another counterindicator for mica was that its coefficient of friction was only 0.033–0.049 at room temperature, while G-10 had a minimum coefficient of friction of 0.33, implying an order of magnitude better ability to carry out-of-plane loads without slippage. The implication of this experiment, in which highly irradiated G-10 was stronger than unirradiated mica, is a counterexample to the supposedly longer irradiation life of ceramics. As will be seen in the discussion on MgO powder, ceramics have endured more irradiation in accelerator environments than organic insulations, but in many applications, organic insulation will be longer lived under intense irradiation. With or without irradiation, the most likely failure mode for either organic or inorganic sheet insulation in a magnetic fusion reactor magnet is powdering of the insulation. A common fear is that

Table III. Properties of MgAl<sub>2</sub>O<sub>4</sub> and Al<sub>2</sub>O<sub>3</sub>

Property	MgAl <sub>2</sub> O <sub>4</sub>	Al <sub>2</sub> O <sub>3</sub> 99.7%	Units
Young's modulus	35	50	Msi
Shear modulus	15		Msi
Compressive strength	270	380	ksi
Bending strength	20–32	50	ksi
Tensile strength	19	30	ksi
Shear strength	9		ksi
Specific gravity		3.94	
Dielectric strength		230	V/mil
Dielectric constant		9.5	

initial cracking of the insulation could lead to shaking out the insulation from between the copper plates by a combination of gravity and the "breathing" of the magnets on each pulse, leading to failure significantly before failure due to the loss of all strength in compression, which Becker showed to occur at very high irradiations for thin disks.

### 3.1.2. Properties of Alumina

Alumina, Al<sub>2</sub>O<sub>3</sub>, is probably the most commonly used ceramic insulation, as well as being the natural insulating coating on all aluminum surfaces exposed to air. It has been used as an insulator in highly irradiated environments in the Triumf septum magnet (see below). Properties of alumina are shown in Table III. According to Clinard (LASL, private comm., 1981), bulk Al<sub>2</sub>O<sub>3</sub> is unusable after an irradiation of  $10^{22}$  (n/cm<sup>2</sup>), because of structural failure due to swelling.

### 3.1.3. Properties of Spinel

Spinel, or MgAl<sub>2</sub>O<sub>4</sub>, has been suggested by J. E. C. Williams (private comm., 1982) as the candidate insulation for FED-R (fusion engineering device-resistive) in the form of a plasma arc sprayed coating, and by Aggarwal et al.<sup>(9)</sup> for the plug magnets in TDF (tandem mirror demonstration facility) in the form of interturn spacer chocks. For an insulation that has never been used in any magnet, it enjoys remarkable agreement at this writing as the most desirable material for high stress, high irradiation applications. Spinel is an attractive ceramic insula-

tion because of its high strength, good thermal conductivity, low neutron swelling, and low solubility in water. Typical mechanical properties of spinel at room temperature are shown in Table III.

Spinel is of particular interest in a high neutron irradiation environment, because of its low swelling. Hurley and Bunch<sup>(52)</sup> irradiated 15 ceramics with a fast-fission spectrum, including  $2.8 \times 10^{21}$  n/cm<sup>2</sup> of  $E_n > 0.1$  MeV fast neutrons. While the (0001)-plane and (1012)-plane slices of Al<sub>2</sub>O<sub>3</sub> experienced identical volume swelling of 1.6% and a reduction of thermal diffusivity of 45%, the single crystal MgAl<sub>2</sub>O<sub>4</sub> had a volume swelling of only 0.1% and a thermal diffusivity reduction of only 8%. However, polycrystalline spinel had a swelling of 0.3% and a thermal diffusivity reduction of 45%. Irradiation was at a temperature of roughly 740 C, and it is likely that radiation damage may have a strong temperature dependence.<sup>(52)</sup> In another set of experiments by Hurley et al.,<sup>(54)</sup> polycrystalline spinel was irradiated to a fast neutron fluence of  $2.1 \times 10^{22}$  n/cm<sup>2</sup> and a thermal fluence of  $4.6 \times 10^{22}$  n/cm<sup>2</sup>, at a calculated temperature of 430 K. In this case, the swelling of the spinel was 0.8%, while the compressive strength was increased from 127 MPa to 152 MPa. The strength of the spinel was five times as high as that of two MgO samples irradiated along with the spinel.

Clinard et al.<sup>(25)</sup> reported the mechanical effects of fast fission neutron irradiation ( $> 0.1$  MeV) from the EBR-II reactor on spinel at 430 K. In single crystals, little gross damage was reported after 30 dpa. In contrast with Al<sub>2</sub>O<sub>3</sub>, hardly any of the defects were aggregated. At 20 dpa, only 0.05% of the total displacements were stabilized in aggregates. The concentration of interstitials contained in loops in MgAl<sub>2</sub>O<sub>4</sub>, expressed as a fraction of the total atoms present, was  $5 \times 10^4$ , after an irradiation of  $2 \times 10^{22}$  n/cm<sup>2</sup>. The failure of loops to unfault and develop into dislocation networks probably explains the superior absence of void swelling in spinel. Vacancy-interstitial recombination is the only important mode of defect accommodation in single-crystal spinel. However, in polycrystalline spinel, excess interstitials reach the grain boundaries, leaving behind an excess of vacancies to agglomerate as voids. While single crystal spinel showed essentially no swelling ( $< 0.1\%$ ) at irradiations from  $0.3$  to  $2.3 \times 10^{22}$  n/cm<sup>2</sup> at high temperatures, polycrystalline spinel swelled by 0.8% after a fast neutron fluence of  $> 10^{22}$  n/cm<sup>2</sup> ( $> 0.2$  MeV) at 430 K. The authors' conclusions are that the

qualitatively different damage mechanism would predict significant differences in the irradiation behavior of single and polycrystalline states of many ceramics, in particular spinel.

### 3.1.4. Properties of Magnesia

Magnesia is the most popular form of powdered insulation, being used in ovens, thermocouples, and accelerator magnets. It has been recommended for use in the bundle divertor magnets of the fusion engineering test facility.<sup>(87)</sup> A particular concern with MgO design in a highly irradiated environment is its photoconductivity under irradiation. Lynch<sup>(69)</sup> tested two MgO coaxial cables over a range of temperatures and irradiation. In each cable the MgO was compacted to 70% of the density of single crystal MgO. One cable had a gamma-induced conductivity of  $1.9 \times 10^{-18} \Omega^{-1} \text{ m}^{-1} \text{ rad}^{-1} \text{ h}$ , while that of the other had a conductivity of  $1.1 \times 10^{-17} \Omega^{-1} \text{ m}^{-1} \text{ rad}^{-1} \text{ h}$ . The lower value corresponds to the photoconductivity of most organic materials, according to Wintle.<sup>(101)</sup>

## 3.2. Comparison of Candidate Organic Insulations for Use in Irradiated Environments

### 3.2.1. Service History

Most large magnets are insulated with epoxy fiberglass composites, in particular G-10. With the exception of the new CR grade, G-10 does not have a fixed composition, although the resin is generally DGEBA (diglycidal ether of Bisphenol A). To the best of our knowledge, the organic insulations with superior radiation resistance, such as TGPAP (triglycidal polyamine phenol) or polyimide resins, have not been used in large magnets. The commonly used high dielectric strength sheet or wrap, Kapton, is also a polyimide, and polyimides are the leading candidate for the insulating chocks in Tore Supra.<sup>(8)</sup>

The NINA quadrupole bending magnets in England are insulated with an imide epoxy and are believed to have been irradiated to several  $10^{10}$  rads with no failures, according to Sheldon, which would be the best known irradiation survival for an organic magnet insulation. The design and construction of the magnets were described by Poole<sup>(82)</sup> before extensive operation had been achieved. The description did

not feature radiation resistance, but stated simply that the coils were wrapped with a layer of woven glass tape, and that a further layer of glass tape was added after winding to give 1 mm of ground insulation. The coil was then vacuum impregnated with a resin designated MY720/HY906, with a permitted operating temperature of 150 C. It was stated that this resin system is the standard choice for magnets at Daresbury, because of its superior physical properties and radiation resistance.

According to Stapleton at Rutherford and Sheldon, several magnets for British and German accelerators have been built by Brown Boveri, using a tetraglycidal amine, similar in its properties to the TGPAP tested by Evans et al.<sup>(35)</sup> and Erez.<sup>(33)</sup> According to Sheldon, the chemical composition of the resin is tetraglycidal diamino diphenyl methane with methyl "medic" anhydride. Both Stapleton and Sheldon state that the insulation, while very good, is difficult to prepare and far from ideal for producing vacuum impregnated coils. Polyimides have been used in irradiated environments, if not in large magnets. According to A. Harvey (private commun.), polyimides used in strain gauges in nuclear reactors are "certainly good" to  $10^{11}$  rads, without failure or sufficient change in electrical properties to invalidate the strain gauge reading. Polyimide varnishes have been used at Los Alamos on 18 gauge wire, wrapped around toroidal particle detectors (A. Harvey, private comm.).

### 3.2.2. Ceramic Insulated Magnets: Service History

The MgO powder insulated conductor, manufactured by Pyrotex of Canada, has been used at S.I.N. in magnets built by George.<sup>(39)</sup> The two most highly irradiated magnets in this class are target area quadrupoles, called QTA and QTB. These magnets used solid mineral filled conductor, externally cooled by steel pipes. The conductor is  $\frac{1}{4}$  in. square and is run at 330 A. The whole magnet was potted in solder. The higher performance internally cooled conductor was rejected because of concern over water erosion of copper. The single most highly irradiated magnet, QTA, was taken out of service after 3 years, due to an electrical blowout. A postmortem revealed no evidence that the failure was in any way related to radiation damage. The target area is believed to have an instantaneous irradiation of  $10^8$  rad/h. The availability of the accelerator was approximately 50% over this period, implying an integrated dose of  $10^{12}$  rad.

### 3.2.3. Screening of Organic Insulations for Radiation Resistance

Materials testing on polyimides, TGPAP, and G-10 suggest that polyimides and TGPAP have a threshold to damage about an order of magnitude higher than that of G-10. A 1970 experiment at the Rutherford High Energy Laboratory<sup>(35)</sup> tested a large number of epoxy resins at dosages up to  $2 \times 10^{10}$  rads. The flexural strength of TGPAP with DDM hardener was 4004 kg-cm<sup>2</sup> preirradiation and 3044 kg-cm<sup>2</sup> after  $2 \times 10^{10}$  rads, which was the threshold to damage irradiation. DGEBA resin with MNA hardener (a typical matrix for G-10) had an unirradiated flexural strength of 3654 kg-cm<sup>2</sup> and an irradiated flexural strength of 1073 kg-cm<sup>2</sup>. The threshold to damage was  $3 \times 10^9$  rads.

Tests at cryogenic temperatures on epoxies and polyimides have been done at Oak Ridge that give more qualitative guidance. Coltman and Klabunde<sup>(26)</sup> irradiated polyimides at 4.9 K, warmed them up to room temperature, and tested their properties at 77 K. Their results appeared with the title, "Mechanical Strength of Low-Temperature-Irradiated Polyimides: A Five to Tenfold Improvement in Dose Resistance over Epoxies." The best glass-filled polyimide was Spaulrad, an aromatic polyimide resin, reinforced by 70 wt-%E-glass fabric, Unirradiated at 77 K, Spaulrad has 90% of the strength of G-10 CR. After an irradiation of  $2.4 \times 10^9$  rads, Spaulrad has five times the strength of G-11 CR, the best irradiated epoxy. By  $10^{10}$  rads, Spaulrad has 38% of its initial strength at 77 K. Norplex, the same material as Kerimid, had the highest strength in compression (800 MPa) perpendicular to the plane of the reinforcement, and this strength did not deteriorate at all up to an irradiation of  $10^{10}$  rads. The simple fact that polyimides are recommended for higher temperature service than G-10 (300 C vs 120 C maximum for G-10) is another qualitative indicator of higher radiation resistance in service, as well as giving more design margin against insulation hot spots.

### 3.2.4. Radiation Resistance of Glass Filler

Tests by Erez<sup>(33)</sup> indicate a strong preference for the use of S-glass in a highly irradiated environment, instead of the somewhat less expensive E-glass, which is most commonly used in unirradiated insulations. Erez irradiated 31 insulator specimens in the M.I.T. reactor to a total fluence of  $1.4 \times 10^{18}$  n/cm<sup>2</sup> and

$5 \times 10^9$  rads of gamma radiation. The activity in mrem/h was measured immediately after irradiation, 3 days and 8 days after irradiation. Typically, the activity with S-glass 901 size was the lowest on all 3 days, being about 1/4 the activity of the systems with E-glass. The activity was essentially independent of the choice of epoxy matrix. Of course, activity *per se* is not a failure mechanism for an insulation, but it is a strong qualitative indicator that less radiation will be absorbed if S-glass reinforcement is used.

### 3.2.5. Price and Availability of Organic Insulations

All three of the candidate insulations are readily available, according to J. Benzinger (Spaulding Fibre, private comm.). A manufacturer's estimate in March, 1982, for the 70,000 ft<sup>2</sup> of 20 mil insulating sheets (based on about 200 sheets for FED-R) is \$9.33/lb for G-10CR with E-glass, \$15.40/lb for G10-CR with S2-glass, \$20.20/lb for TGPAP with S2-glass, and \$38.80/lb for the polyimide Spaulrad with S2-glass. The TGPAP resin comes in two grades: a distilled resin, available at \$14.50/lb, and the regular grade, available at \$6.55/lb, which was used in the composite costing. The prices quoted were for 20 mil sheets, suggested by the experiments by Becker in which thin disks had substantially higher irradiated fatigue life than thick disks. However, due to the manufacturing difficulties associated with thin sheets, the cost of 40 mil sheets was estimated to be only slightly higher than that for 20 mil. In all three cases, the insulation would be 70 wt-% S-glass. This gives a price range of \$500,000 for the polyimide composite to \$120,000 for the G-10 composite with E-glass.

Although Benzinger stated that polyimides and TGPAP are much less available than G-10, he also told Erez and Becker that the delay for polyimides would be about a week for the Zephyr TF plates,<sup>(102)</sup> which are about 1/2 the surface area of the FED-R plates. Presumably, the delay is just the time it takes a boat from France to make a delivery from Rhone-Poulenc, and is not a strong function of quantity. Another attractive polyimide resin, Kerimid, is manufactured by Rhone-Poulenc. According to Erez (M.I.T., private comm.), two fabricators in the United States are capable of manufacturing laminated sheets large enough for the Zephyr TF magnet plates.<sup>(102)</sup> According to manufacturer's literature, this resin has been used as a structural material in nuclear reactors, with no damage at irradiations up to  $10^{10}$  rad, and

has a flexural strength of 70 ksi and a compressive strength of 50 ksi.

According to J. Dyer at Atlantic Laminates (private comm.), 36×48 in. is the standard sheet size of Kerimid, and it could be fabricated in sizes ranging from 4–5 mils to 1 in. thick. However, Atlantic Laminates does have a 48×72 in. press, which can only be heated to 250 F. The curing temperature of the polyimide is 425 F, so final curing would have to be done in a separate oven, but Dyer believes that this is feasible. Another limitation is that woven glass cloth is available only in rolls no larger than 50 in. Dyer said that an overlap between two sheets of cloth could be cushioned without damaging the press, although the flexural strength of the composite would be greatly reduced at the overlap plane.

### 3.2.6. Availability and Limitations of Powdered MgO Insulated Conductor

Powdered MgO insulated conductor is currently the only conductor with proven long life in a highly irradiated environment. It is used at the LAMPF facility in Los Alamos<sup>(43)</sup> and at the Schweizerisches Institut für Nuklearforschung (SIN) in Villigen.<sup>(39)</sup> All conductor to these two facilities has been delivered by Pyrotenax of Canada. Presently, the available size and current density of this type of conductor is very limited. Although there are also fundamental limits on conductor performance of this technology, primarily because of the need for an external jacket, as well as limitations on conductor bending radius, present size and performance limitations reflect primarily the small size of the market for this conductor. According to D. Main (private comm.), Pyrotenax has supplied conductors to scientific laboratories in the United States, particularly the LAMPF facility at Los Alamos, and abroad in sizes up to 0.35 in. flat-to-flat on the copper, 0.53 in. overall for a solid conductor, 0.75 in. flat-to-flat in the coolant hole, 0.57 in. on the copper, and 0.75 in. overall for a hollow water-cooled conductor. The latter conductor is rated at 1800 A and is manufactured in 230 ft lengths.

The manufacturing process used by Pyrotenax is to draw a 2.5 in. o.d. copper sheath to approximately the correct size and then to square the conductor, with, perhaps, some more drawing. It is necessary to leave a  $\frac{1}{4}$  in. gap between the conductor and the sheath, in order to fill the conductor gap with MgO

powder. This is apparently a fundamental limitation on the space taken up by the insulation. For a fusion reactor application, where a high current is desired, it would probably be possible to just square up the original 2.5 in. o.d. pipe. The manufacturer recommends not bending the conductor to a radius of less than 12 times the conductor width. Main observed that at least one coil wound at LASL can be seen to be bent to a radius less than that, but he cautions that if we used the original 2.5 in. o.d. pipe, it would probably not be very flexible and that the original rule of thumb should apply. An undrawn conductor would only be available in a maximum length of 30 ft. Main said that no conductors have been manufactured with coolant channels between the current-carrying copper and the MgO insulation. If that topology were used, thermal runaway should not be a problem in the insulator, and only bending radius and the avoidance of temperatures above 250 C in the copper would limit the conductor current density.

Main reports that the largest cable that Pyrotenax can manufacture with their present technology is 2.07 in. flat-to-flat, where the included copper conductor is 1.63 in. flat-to-flat and the jacket thickness is  $\frac{1}{16}$  in. A minimum bending radius of 24 in. is recommended. The failure mode due to overbending is rippling of the jacket inside surface. Main said that the coil could probably be manufactured with a stainless-steel jacket, if desired. The coolant hole can be made any reasonable size desired. Main confirmed the manufacturer's literature that 250–300 C is the design limit due to oxidation of the copper.

### 3.3. Neutron and Ionizing Radiation Damage to Copper

#### 3.3.1. Lattice Displacements

The resistivity of copper is increased by irradiation through the introduction of defects into the copper lattice. These defects include the transmutation of copper into other elements, and the introduction of voids, dislocations, and intrinsic point defects, such as vacancies and interstitials. According to T. H. Blewitt (private comm.), almost all neutron energy is lost by elastic collisions. About 95% is lost in heat and 5% in defects. Of the 95% lost in heat, 85% is due to ion-ion interactions and 10% to electron excitation. The mean free path of a high-energy neutron in copper is about 1 cm. About half of the collisions will

cause excitations and half displacements. A 2 MeV neutron will require about 500 collisions to thermalize in copper. The scattering angle will be nearly arbitrary, with only a slight tendency for a neutron to make forward progress in its initial direction.

A rough conversion between dpa (displacement/atom) and appm (atomic parts per million of an impurity) is made as follows: the neutrons in a typical fusion first-wall spectrum may typically experience 400 matrix displacing collisions (400 displacements) before being captured (1 impurity atom). This was the ratio in the RTPR reference design.<sup>(24)</sup> A direct fusion neutron should cause about 1200 displacements. Therefore, at low integrated fluences and low temperatures, there are approximately 400 displacements/impurity. However, at room temperature about 85% of the defects will be annealed out at steady state. At the most elevated of possible magnet temperatures (250 C), about 95% of the defects will be annealed out. Each transmutation causes an increment in the copper resistivity 3–4 times greater than the increment from each displacement. Therefore, for an unsaturated matrix, the effect of displacements may be less than an order of magnitude greater than the effect of transmutations. At room temperature, the copper matrix will only support about 0.1% defects. Above the fluence necessary to produce the saturation level of lattice defects, only the resistivity due to transmutations continues to increment. At room temperature, the incremental resistivity due to lattice defects is no more than  $3 \times 10^{-9}$   $\Omega$ -m. At room temperature, the additional resistivity due to point defects saturates at  $0.34 \times 10^{-8}$   $\Omega$ -m.<sup>(48)</sup> T. H. Blewitt (private comm.) reports that there is an overall upper bound of a resistivity increase of  $4.0 \times 10^{-7}$   $\Omega$ -m due to lattice defects, after which the lattice won't support any more defects. A rule of thumb is that the resistivity of copper at room temperature or above increases at a rate of 1%/300 appm. The thermal conductivity decreases at the same rate.

#### 3.3.2. Transmutation of Copper

Transmutation of the elements in magnets occurs in fusion reactors, because of the copious production of neutrons by deuterium-tritium reactions. The cross-section graphs in Garber and Kinsey<sup>(37)</sup> showed that (n,2n) reactions in copper peak at about 14 MeV. Weighted over the two principle isotopes  $^{63}\text{Cu}$  and  $^{65}\text{Cu}$ , this reaction has an equivalent

cross-section of 1 barn. According to T. H. Blewitt (private comm.), transmutations occur primarily at thermal velocities, because at room temperature, the absorption cross-section is 3.69 barns, while the scattering cross-section is 7.2 barns. Between 1 and 100 eV, the total cross-section is nearly constant at 7–8 barns. Since the scattering cross-section does not change much with neutron energy in this region, the absorption cross-section must be reduced below 1 barn. Copper does have resonance absorption peaks at epithermal energies below 1 Mev, but Blewitt said that the areas under those peaks is small.

### 3.3.3. Mechanical Effects of Radiation on Conductor

Glowinski found that the peak swelling range for copper is from 500 to 775 K, with a peak at 625 K and an initial swelling rate at that temperature of 0.4 vol%/dpa. Saturation effects may set in before a damage level of 30 dpa is reached. Blewitt states that copper is strengthened by irradiation, at least up to 400 K. Blewitt (private comm.) states that there should be no significant loss of ductility in copper (or any other metal with face-centered-cubic crystals) up to a fluence of  $10^{20}$  n/cm<sup>2</sup>. Blewitt had irradiated pure copper crystals to an irradiation of  $10^{22}$  on the HIFR reactor, and the yield strength was nearly the same as in the unirradiated case at room temperature.

### 3.3.4. Blistering

Blisters can form in copper, due to helium trapping. In a fusion magnet, no magnet component would be in direct contact with helium produced by the fusion reaction. However, helium can form within the copper conductor, due to  $\text{Cu}^{65}[(n, n\alpha) + (n, \alpha n)]\text{Co}^{61}$  reactions. Terreault et al.<sup>(95)</sup> found a sharp threshold for blistering of  $4 \times 10^{17}$  He/cm<sup>2</sup> in copper foil under irradiation by 20 keV helium ions.

## 3.4. Radiation Damage Mechanisms in Insulation

Neutron irradiation causes swelling in ceramics, which is probably the dominant long term cause of failure. Neutron, gamma, and X-radiation break organic bonds in organic insulators, as well as evolving trapped hydrogen and helium gas. Based on measurements in Al<sub>2</sub>O<sub>3</sub>, the accumulation of defects in a ceramic due to neutron irradiation is expected to

proceed at a rate of

$$\text{appm}(\text{H} + \text{He}) \approx 0.6 \times 10^{-19} \Phi$$

where appm is the atomic parts per million of hydrogen and helium in the ceramic, and  $\Phi$  is the integrated neutron fluence in n/cm<sup>2</sup>; thus

$$\text{dpa} = 0.8 \times 10^{-21} \Phi$$

where dpa is the total number of lattice displacements per atom.

### 3.4.1. Electrolysis

At elevated temperatures in an electric field, a ceramic insulation can be destroyed by electrolysis, the migration of impurity ions within the body of the ceramic. Narayan et al.<sup>(75)</sup> investigated  $1.5 \times 1.5$  cm samples of single-crystal MgO at 1273 K. The maximum dc electrical field was 1000 V/cm. Catastrophic breakdown occurred after periods ranging from 5 to 150 h. Since diffusivity is typically enhanced by irradiation, it is anticipated that a significant neutron flux will accelerate electrolysis. Weeks tested Al<sub>2</sub>O<sub>3</sub> and didn't find evidence of electrolysis at temperatures up to 800–1000 C. According Weeks also found that, even under intense neutron irradiation, a magnet insulator operating at the relatively low temperatures typical of magnets (< 300 C) should not exhibit significant electrolysis. Weeks's experiments were performed on single-crystal samples; it is possible that iron migration will be significantly worse along grain boundaries in polycrystalline bulk ceramics.

### 3.4.2. Photoconductivity

The conductivity of any insulation is increased by ionizing radiation, due to the excitation of valence electrons across the band gap into the conduction band. This mechanism and the consequences for highly irradiated magnet design have been reviewed by Perkins.<sup>(79)</sup> Van Lint reviewed the data on photoconductivity and concluded that a linear relation between dose rate and additional conductivity existed where the proportionality constant ranged between  $10^{-9}$  and  $10^{-13}$  ( $\Omega\text{-m}$ )<sup>-1</sup>/(Gy/s). The proportionality constant is a function of the material, the temperature, and the integrated fluence.

Lynch<sup>(69)</sup> measured the photoconductivity of two MgO coaxial cables over a range of temperatures and irradiation. In each cable the MgO was compacted to 70% of the density of single crystal MgO. One cable had a gamma-induced conductivity of  $1.9 \times 10^{-18} \Omega^{-1} \text{ m}^{-1} \text{ rad}^{-1} \text{ h}$ , while that of the other had a conductivity of  $1.1 \times 10^{-17} \Omega^{-1} \text{ m}^{-1} \text{ rad}^{-1} \text{ h}$ . The increase was an order of magnitude greater than that measured by Davis<sup>(29)</sup> in solid ceramic. F. Clinard (LASL, private comm.) suggested that the increase in conductivity may be due to ionization of the trapped and compressed gas in the powder matrix.

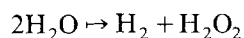
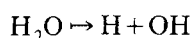
### 3.4.3. Swelling

George Hurley at LASL expressed the opinion that swelling in a MgO powder could be life-limiting. Hurley observed 4% swelling at  $2 \times 10^{22}$  fission neutrons ( $\approx 1 \times 10^{22}$  fusion neutrons) at elevated temperatures. (There are hardly any data on room-temperature irradiation of ceramics; 335 C is about the lower limit.) At lower temperatures, a fairly low dose ( $10^{20} - 10^{21} \text{ n/cm}^2$ ) of neutrons swells either MgO or  $\text{Al}_2\text{O}_3$  to 1%, but then saturates. Because of the low packing factor of ceramic powder insulation ( $\approx 95\%$ ), along with the long service lives reported above, it is not clear that swelling is a life-limiting mechanism for ceramic powders, in the way that it is for bulk ceramics. If it is not, then there are probably no life-limiting mechanisms associated with neutron damage *per se* for the powdered ceramic insulations for any reasonable fusion or accelerator application, with the possible exception of electrolysis.

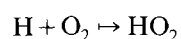
## 3.5. Radiation Effects on Water

### 3.5.1. Radiolysis

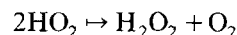
The main initial decomposition reactions of irradiation on pure water are



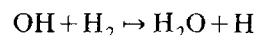
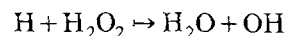
The formation of  $\text{H}_2\text{O}_2$ , hydrogen peroxide, is largely dependent on the presence of free molecular oxygen in the water, which is the dominant acceptor of atomic hydrogen, through the reaction



followed by



The back reaction of the reaction products to reform water can be formulated as



The presence of solutes can protect the initial decomposition products by destroying the free radicals by oxidation-reduction reactions, allowing hydrogen to evolve and hydrogen peroxide to decompose. Since solute molecules vary considerably in specificity of reaction, several orders of magnitude differences can be obtained in decomposition product concentrations when different aqueous solutions are irradiated. The steady state concentration of hydrogen peroxide is also a strong function of pH, with alkaline pH favoring a lower  $\text{H}_2\text{O}_2$  concentration.<sup>(100)</sup> Radiation induced chemical reactions in pure water are reversible. Borated water will evolve gas irreversibly as a linear function of neutron scattering and capture. However,  $\gamma$ -energy absorption favors the back reaction. Antifreeze solutions will decompose extensively under irradiation.<sup>(34)</sup> An extensive review of the unclassified data available on the decomposition of water is summarized by Etherington.<sup>(34)</sup> Unfortunately, a typographical error omits the reference. The major conclusions are:

1. Under the average neutron-gamma flux levels existing in cooling water of present nuclear reactors, the instantaneous decomposition rates and the maximum concentrations of decomposition products are very close to zero for initially gas-free, relatively pure water. An initial purity of  $10^6 \Omega\text{-cm}$  or higher is recommended, and can be achieved by the use of a bypass, mixed-bed ion-exchange system.
2. Increased temperature results in reduced decomposition rates and equilibrium concentrations of decomposition products. Above 300 F, the recombination rate is high and essentially independent of temperature.
3. At low temperature, decomposition is so repressed by excess hydrogen that virtually no decomposition occurs at average neutron and gamma irradiation levels in present reactors if hydrogen equivalent to 5 to 10 psi partial pressure is initially



Table IV. Liquid Water Radiolysis by  $\gamma$ -Rays

Dose rate	$10^{17}$ – $10^{20}$ eV/(g-s)
Additives	None
pH	3–13
G(-H <sub>2</sub> O)	4.45 molecules/100 eV
G(H <sub>2</sub> )	0.4 molecules/100 eV
G(H <sub>2</sub> O <sub>2</sub> )	0.63 molecules/100 eV
G( $e_{aq}^-$ )	2.63 electrons/100 eV
G(H)	0.55 radicals/100 eV
G(OH)	2.72 radicals/100 eV
G(HO) <sub>2</sub>	0.026 radicals/100 eV

dissolved and maintained in otherwise relatively pure water.

In 1944, Weiss attempted to show that the much larger body of knowledge of photochemistry of solutions could be applied directly to the radiochemistry of aqueous solutions.<sup>(100)</sup> The rate of disappearance of any arbitrary solute acceptor molecule would then be given by the equation:

$$-\frac{dS}{dt} = \frac{\kappa k_{S+OH} R_{abs} [S]}{k_{H+OH \rightarrow H_2O} [H] + k_{S+OH} [S]}$$

where  $k_2$  and  $k_S$  are rate constants,  $R_{abs}$  is the total radiation absorbed per unit of time,  $\kappa$  is a proportionality factor, and bracketed symbols are concentrations in g-mol/L. The rate of radiolytic production of water reaction products is summarized by Prelas et al.<sup>(83)</sup> and given in Table IV. The steady-state concentrations of radiolysis breakdown products in initially pure water, calculated by Boyd et al.<sup>(14)</sup> and measured by Schwarz<sup>(88)</sup> can be expressed by the correlations:

$$H_2O_2 + O_2 \left( \frac{\text{mol}}{\text{L}} \times 10^6 \right) = 1.83 \times 10^{-10} \sqrt{\Phi}$$

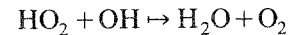
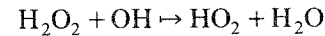
and

$$H_2O_2 \left( \frac{\text{mol}}{\text{L}} \times 10^6 \right) = 0.719 \times 10^{-10} \sqrt{\Phi}$$

where  $\Phi$  is the energy deposition flux (eV/L-s).

The combined effect of neutrons and gamma radiation on water and aqueous solution decomposition in a reactor pile was measured by Allen.<sup>(1)</sup> Allen discovered that the ratio of hydrogen peroxide to total oxidant, i.e., oxygen and hydrogen peroxide,

decreased from 0.99 at to an exposure time of 0.001 h to 0.2 at 100 h. This suggests that the principal oxidizing agent for long term corrosion may be oxygen, rather than hydrogen peroxide. Allen suggested the following reactions to explain the decomposition of hydrogen peroxide to oxygen:



### 3.5.2. Water Transmutations

During nuclear reactor operation, the major radioactivity in the water is due to N<sup>16</sup>, formed from O<sup>16</sup> in H<sub>2</sub>O, and N<sup>17</sup> formed from O<sup>17</sup>. Short-lived activity of 0.3  $\mu$ Ci/ml has been reported in the Naval Reactor Test Facility.<sup>(17)</sup> The water transmutation and longer lived radioactive corrosion products in the water are probably the greatest environmental hazard of highly irradiated magnets, but should not affect the magnet lifetime.

### 3.5.3. Radiolytic Corrosion

The mechanisms of oxidative corrosion were reviewed by Dorra<sup>(31)</sup> in order to elucidate the additional mechanisms of corrosion due to radiolysis. Chemical corrosion by water occurs because of the natural contact potential between copper and water, caused by the greater mobility of electrons in a metal than in water. This leads to a diffusive drift of copper ions towards the copper-water interface. The electric potential causing copper diffusion is higher, the higher the oxygen content of the water is. Electrons, reaching the surface first, join with oxygen in the water to form copper oxide at the surface. The excess of electrons forms the familiar sheath potential, which inhibits further oxidation. However, any sink for electrons, such as a voltage, chemical reactions, or radiation effects, can cause steady corrosion through the sheath. The separation of terms of different corrosion causes is extremely difficult, because the corrosion process is complex and is simultaneously a strong function of temperature; water velocity and/or Reynold's number; water pH; and in particular, the oxygen content, content of metal impurities other than copper, and radiation dose.

While some authors use the terms erosion and corrosion interchangeably, Dorra considers erosion to

be the diffusion of copper into water in the total absence of oxygen. He then divides the corrosion mechanisms into four dominant regimes.

1. *Erosion dominated-oxygen level = 0.* In the erosion dominated regime, there is no corrosion. This limit is theoretical, since oxygen can enter the system through whatever air is adsorbed by surfaces in the cooling circuit, particularly organic materials. Without some sort of degassing apparatus, the corrosion rate of initially pure water will rise rapidly. At the lowest concentrations of oxygen, corrosion can be high again, due to the loss of the copper oxide coating. This can be cured by the addition of either hydrogen or helium to the water.

2. *Erosion dominated-oxygen level < 50 ppb.* Below an oxygen level of 50 ppb, corrosion exists, but erosion still dominates. The conductivity of the water increases slowly and can mainly be accounted for by the erosion rate. The conversion between erosion and conductivity in the regime in which recombination is negligible, i.e., most of the copper is in solution as  $\text{Cu}^{2+}$ , is given by Landolt and Börnstein<sup>(64)</sup>:

$$\sigma = \frac{3.43 \times 10^{-6}}{\rho_{\text{Cu}}}$$

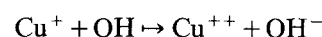
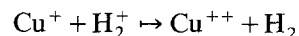
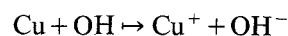
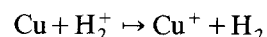
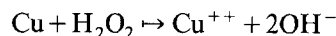
where  $\sigma$  is the water conductivity (S/cm), and  $\rho_{\text{Cu}}$  is the copper ion density (ppb). The presence of other ionic species in the water can invalidate the above relation, which can only be considered valid in water with a resistivity below  $0.16 \mu\text{S}/\text{cm}$  at 25 C, according to Dorra.<sup>(31)</sup>

3. *Oxide coating dominated-500 ppb < oxygen level < 2000 ppb.* In this regime, the majority of the copper ions leaving the bulk copper go to building the oxide coating. Chemical combination of copper with cations in solution also becomes significant in this regime.

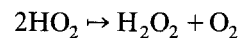
4. *Recombination and deposition dominated-2000 ppb < oxygen level < 8000 ppb.* In this regime, it is essentially impossible to separate the various corrosion mechanisms. The chemical combination rate is the highest in this regime, and the danger of cooling channel stoppage because of deposition becomes great. The conductivity of the water stops rising in this regime. The corrosion rate also ceases to have a first-order dependence on the oxygen concentration.

The presence of radiolytic breakdown products in water, particularly hydrogen peroxide, can be

expected to accelerate the erosion of copper or insulation described above in the section on erosion. Radiolytic corrosion of copper has been observed in accelerator cooling systems<sup>(48a)</sup> and in an accelerator simulation by Hoyer.<sup>(49)</sup> The corrosive reactions that occur in the presence of hydrogen peroxide are

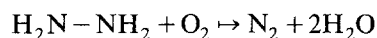
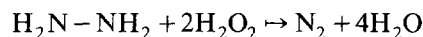


The principal results are that mainly doubly-charged copper is formed and that its concentration solution increases, as does the pH of the solution due to the formation of  $\text{OH}^-$  ions. In addition, hydrogen and oxygen gas are formed by the decomposition of hydrogen peroxide and by the reaction



until the water is saturated with oxygen at approximately 8 mg  $\text{O}_2/\text{L}$ . After that, the increase of the hydrogen peroxide net concentration is a linear function of the absorbed dose.<sup>(3)</sup>

Von F. Hoyer simulated the irradiation conditions in the cooling circuits of a proton accelerator at CERN by irradiating a simulation chamber filled with copper plates with the 600 MeV CERN synchrotron. The simulation chamber was simply a box of copper plates with more surface area and less volume than the cooling circuit of interest. The effect of the corrosion inhibitors hydrazine and benzotriazole was studied. Hydrazine is expected to inhibit corrosion by combining with the oxidizing agents and removing them from the water:



Benzotriazole is expected to inhibit corrosion by forming insoluble copper complex precipitates in the form of surface layers on the copper. In Hoyer's experiment, hydrazine had only reduced the  $\text{Cu}^{2+}$  concentration after 10 h of irradiation by a factor of 1.3 versus the concentration in originally pure water, while benzotriazole reduced the concentration after

10 h by a factor of 2. If the corrosion of copper and insulations by water is too severe, a steel cladding might be used. Typical corrosion rates observed for types 347 and 304 steels are 0.06 mil/yr in nuclear reactors.<sup>(17)</sup> According to M. A. Schultz (private comm.), borated H<sub>2</sub>O is run routinely in nuclear reactors at 30 ft/s through steel or zircalloy claddings, without undue corrosion. Stainless steel claddings as thin as 5 mils are practical.

#### 4. HIGH PERFORMANCE MAGNET DESIGN

Several magnet laboratories around the world have built high stress, high heat flux, high field magnets, usually for the purpose of solid state physics investigations. Most of these magnets use either the simple Bitter plate construction or the theoretically higher performance polyhelical magnet construction. The achievements of these high field magnets were recently summarized by Bazan.<sup>(10)</sup> According to Bazan, the only significant improvement in performance, as measured by central field, has been in recently constructed hybrid magnets, using an outer superconducting solenoid.

##### 4.1. Bitter Magnets

The helical arrangement of thin plates or disks into a pressure joined stack, invented by Francis Bitter, is probably the most popular method of fabrication for high-performance, high-field magnets. The Bitter topology is inherently strong in bending, well-cooled, and relatively easy to assemble. Its fundamental disadvantage is a poor theoretical recirculating power and volume requirement for a given central field and bore size, when compared with independently supported and charged concentric coils. Another disadvantage, when compared with internally cooled conductors, is that it has not demonstrated a capability for long life when water is the coolant, because of the life-limiting effects of water contact with the insulation and joints. This class of failure mechanisms is discussed below in the section on the work of FBNML. The theoretical limitation of uneven stress and current density in the magnet can be reduced significantly, with only a moderate increase in magnet complexity, by stacking two concentric Bitter magnets, as in the design of the 3.3 cm bore 30 T hybrid magnet<sup>(67)</sup> at M.I.T. and the 25 T hybrid magnet [HU81] at Nijmegen.<sup>(55)</sup>

A possible solution to the life-limiting mechanism of occlusion of coolant passages by the motion of insulating sheets is to bond the insulating sheets to the copper disks. This has been done by Katrukhin et al.<sup>(59)</sup> in moderate performance (12 T) Bitter solenoids at the L. V. Kirensky Institute of Physics in Krasnoyarsk, USSR, and the International Laboratory for High Magnetic Fields and Low Temperatures in Wroclaw, Poland. Operating as the insert coil of a hybrid magnet at Kirensky, a central field of 19.5 T was achieved. The coils consist of stacked composite blocks of copper and insulator, in which coolant channels are bored after glueing. Overlaps are sized to make good electrical contact, even in the absence of external pressure. The overlap surfaces are copper-plated up to 35  $\mu\text{m}$  and silver-plated up to 5  $\mu\text{m}$ . The main disk surfaces are silver-free and are oxidized, followed by priming with epoxy-silicone. The turn-to-turn insulation is a 0.08 mm glass fabric, impregnated with an epoxy-phenolic adhesive. Before impregnation, the glass fabric is treated in 1% silicone solution, in order to improve the resistance to wetting. Several copper-insulator composites are formed at once under axial pressure in an oven, baking a stack of disks at 170 C for 10–12 h. Deburring is done by chemical etching. It is claimed that the operating temperature of the magnet is limited only by annealing of the copper at 150 C, and not by any degradation of the insulation properties. Coils are routinely reconditioned, by chemically etching the magnets to remove copper oxide from the coolant channels.

##### 4.2. Polyhelix Magnets

Polyhelix magnets consist of a number of coaxially nested thin coils which are mechanically independent of each other. The advantage of this approach over Bitter magnets is that one can design for equal stress in each helix, thus allowing higher overall current density and less recirculating power for a given central field. The radial current distribution needed to give constant stress in a solenoid and in a trapezoidal magnet was derived by Schneider-Muntau and Rub<sup>(89)</sup> to be

$$j(r) = \frac{a_1}{r} \left[ \frac{B_0^2}{\sigma\mu_0\lambda} + 2 \ln \frac{a_2(b + \sqrt{r^2 + b^2})}{r(b + \sqrt{a_2^2 + b^2})} \right]^{-\frac{1}{2}}$$

for the solenoid. This gives a Fabry factor about 20% better than the  $1/r$  current density of Bitter solenoids at high values of  $\alpha$ , the ratio of the outer to inner radius.<sup>(89)</sup>

## 5. CASE HISTORIES

### 5.1. Design Practice: Major Systems Under Construction

#### 5.1.1. TFTR

The Tokamak Fusion Test Reactor at the Princeton Plasma Physics Laboratory includes 20 toroidal field coils with a total weight of 1.2 million pounds. These magnets are essentially unshielded from the neutron production by deuterium-tritium reactions in the tokamak plasma. The coils for TFTR are relatively conservatively designed and represent a good indicator of present design practice for large, water-cooled copper magnets. A typical EF conductor is  $\frac{1}{2}$  by 3 in. copper with a  $\frac{1}{4}$  in. slot milled in the top of the conductor. A cooling pipe is soldered into the slot. The toroidal field turns vary from  $1.2 \times 1.1$  in. with a  $\frac{1}{2}$  in. diameter hole in the center to  $1.1 \times 1.9$  in. with a  $\frac{1}{2}$  in. diameter hole in the center. The maximum design temperature in the copper is only 120 F. The system pressure drop in the water pumping system is 6 atm, and the maximum inlet temperature is 85 F. It was found by experiment that there was a 20% degradation of strength in the vacuum impregnated insulation at 150 F. Considerable effort was made in the design of the overall coil support system to reduce the interturn shear in the insulation, which was felt to be the critical mechanical design issue.<sup>(12)</sup> The final design reduced the interturn shear from an original value of 45 MPa (6.6 ksi) to 22 MPa. The allowable level was selected to be 40 MPa.

#### 5.1.2. JET

The Joint European Tokamak at Culham, England, is a deuterium-tritium burning tokamak experiment. Its toroidal field system is made of 32 identical D-shaped coils.<sup>(81)</sup> Each coil consists of 24 turns of 66.4 kA conductors, arranged as two 12 turn pancakes. The sides of the conductors are machined to form a trapezoidal winding cross-section in the throat of the toroidal magnet system. The peak design cur-

rent density in the smallest of the conductors is 2.7 kA/cm<sup>2</sup>, which is very high for such a large, internally cooled conductor in a wound magnet. The magnet design includes several advanced features which permit this high performance. There are two extruded coolant holes in each conductor, reducing the temperature drop across the copper for a given copper and coolant area. Interlocking keyways between each turn are filled with insulation in order to protect against shear failure of the interturn bond. Each turn is cooled in parallel with every other turn, in order to minimize interturn thermal stresses. The flow rate of water through one coil is 37 L/s.

The maximum turn-to-turn voltage is 12 V/turn, withstood by a 2 mm vacuum impregnated epoxy resin-glass system (6 V/mm). The maximum voltage between pancakes is 281 V, withstood by 6 mm of the same insulation system (47 V/mm). The maximum supply voltage is 9 kV, withstood by 7 mm of the insulation system (1280 V/mm). The center point of each coil is grounded, so the maximum voltage between the conductor and ground is only 4.5 kV, except in the case of a ground fault. Each turn is made from a single length of copper conductor to form one water cooling circuit, which is brazed to a water connection block in the top, outer region of the coil. The interpancake electrical connection is also made in this region. The coils were wound in the so-called constant-tension D shape, requiring a straight section in the throat. Winding the coil under a tension equal to the tension under load over a concave block was necessary in order to prevent further deformation of copper under load and to provide a straight section following postwinding springback of the conductor. Three trials were necessary before the final shape assumed by the conductor was satisfactory.

JET reported a manufacturing limitation of 4000 mm<sup>2</sup> for copper with two internal coolant channels from Kabelmetal of Osnabruck.<sup>(13)</sup> JET was able to obtain their conductor in 15 m lengths, corresponding to the length of a single turn. This involves the use of a 5000 ton extrusion press, starting with a 1000 kg billet. One of the two competing manufacturers was eliminated because samples were too difficult to braze, due to drawing lubricant being trapped in the joint connecting the two water channels. The poloidal coil system in JET includes four groups of circular dipole coils with an iron transformer core.<sup>(65)</sup> The total weight of these coils is 350 tons and the largest coil is 10.9 m in diameter.

Table V. Properties of Magnet Coil Insulation System Orlitherm OH67

Properties	Units	Pure resin	Composite insulation
Mechanical			
Flexural strength at 23 C	N/mm <sup>2</sup>	80–120	400
Shear strength, insulation to copper	N/mm <sup>2</sup>		up to 50
Physical			
Density	g/cm <sup>3</sup>	1.2–1.25	1.8–2.0
E modulus at 20–130 C	N/mm <sup>2</sup>	$3 \times 10^3$	$1-2 \times 10^4$
Thermal			
Maximum operating temperature	C	130	155
Martens temperature	C	110	
Electrical			
Puncture strength at 50 Hz, 23 C	kV/mm	20	25–30
Dielectric constant at 50 Hz			4.5–5.0
Irradiation resistance			
Decrease to 50% of flexural strength	rad	$1 \times 10^9$	up to $10^{10}$

The maximum power supply voltage at the terminals of the poloidal field coils is 40 kV (20 kV to ground). It was felt that an epoxy/glass insulation would have inadequate reliability at this voltage. Mica/glass/epoxy was tested and found to have insufficient shear strength. An insulation system using interleaved glass tape and polyimide (Kapton) tape was developed. The coils have 1 mm of this insulation wrapped on each conductor, including 1 layer of Kapton and 2 of glass, and 6–8 mm of ground of insulation, including 6–8 layers of Kapton and 12–15 layers of glass.

The rationale for the insulation selection for JET is given by Koch et al.<sup>(63)</sup> The basic requirement was to find an insulation system with high shear, compression fatigue strength, high dielectric strength, and high radiation resistance. B-stage epoxy systems were rejected because of their limited shear strength. The epoxy resin system selected was Orlitherm OH67, a Bisphenol A (F-type) epoxy resin, with MNA hardener. The system has low viscosity and relatively low reactivity at 90 C, allowing long pot life and densely packed insulation. The reinforcement of the resin is made with Silan sized dry glass-fabric, because of its high mechanical strength and high radiation resistance. The high voltage requirement of greater than 10 kV is met by incorporating an elastic plastic film of Kapton, which bonds well to the Orlitherm resin. Tests at CERN<sup>(72)</sup> showed that the flexural strength and Young's modulus did not decrease by 50% until after an irradiation of up to  $10^{10}$  rad of the glass reinforced insulation. A table of coil insulation properties is shown in Table V.

### 5.1.3. JT-60

JT-60 is a large tokamak experiment, built in Japan by the Japanese Atomic Energy Research Institute (JAERI). The toroidal field magnets are similar in size and performance to those of TFTR. The JT-60 toroidal field magnet system uses 18 coils with a maximum field of 9.8 T, a total system current of 67.5 MA-turns, and a stored energy of 2.85 GJ. Each coil consists of two wedge-shaped pancakes of 72 turns. The inside radius of each coil is 1.94 m, while the outside radius is 2.86 m. Each conductor carries 52 kA with a flat-top length of 5 s, and an equivalent square-pulse time of 38 s, with a maximum current density at the peak of the nose wedge of 2.68 kA/cm<sup>2</sup>. The peak terminal voltage of a coil is 7.5 kV.

Each turn of the winding has two parallel water cooling circuits. The maximum temperature rise of the conductor is up to 70 C in the wedge, and the maximum temperature difference between two adjacent turns is less than 5 C. The circuits are not internal to the conductor, as in the JET design, but are into a single notch in each conductor. A higher resistivity, higher strength copper alloy (0.2 w/o Ag-OFE at 40% reduction) is used in the high stress region near the center support of the magnet. This is connected to a purer copper by brazing each turn at the top and the bottom of the coil block. The yield strength of the silver alloy is 372 MPa, while the decrease in conductivity is 2%. The magnets are designed to a maximum stress intensity of 216 MPa (31 ksi) in the conductor and 372 MPa (54 ksi) in the structure.

The turn-to-turn insulation is 1 mm F-stage epoxy, while the ground insulation is 10 mm. The 1 mm layer insulation consists of a polyamide sheet and two nonwoven glass fibers on each side of the sheet, prepregnated with epoxy resin. The 10 mm ground insulation is composed of a main insulation layer of mica and a protection layer of glass fiber, which are also prepregnated with epoxy resin. The specimens of the ground insulation showed breakdown voltages of 60 kV at 1000 cycles to 35 kV at  $1 \times 10^6$  cycles.

## 5.2. Operating Experience: High Performance Magnets

### 5.2.1. Francis Bitter National Magnet Laboratory

At the Francis Bitter National Magnet Laboratory at M.I.T., several high-field Bitter magnets and higher-field hybrid magnets (superconducting magnets with normal, Bitter magnet inserts) have been constructed. The stand-alone Bitter magnets have bores ranging from 3.2 to 24.8 cm and central flux densities from 7.5 to 23.4 T. The magnets at the laboratory have a bore field-squared product of about  $B^2D = 20T^2 - m$ . According to R. Weggel,<sup>(99)</sup> the usual design practice at FBNML is to design Bitter solenoids to overall stresses of 25 ksi across a magnet cross-section. Most of these high stress, high field magnets are deliberately fatigue-life limited, because they are inexpensive and are used to produce state-of-the-art magnetic field regimes. Typically, the water flow velocity is in the range of 8–10 m/s. The dominant failure mechanism involves water damage to the insulation, since the insulation must be in direct contact with cooling water in Bitter magnet construction. Typical lifetimes have been reported to lie within the range of 200–1000 MWh, corresponding to an integrated operating life on the order of 1000 h. A hollow conductor, providing the first 4 T of a Bitter-wound coil hybrid, has been operated to 10s of 1000s of hours at an operating stress of about 5 ksi and coolant velocity of a few m/s.

According to J. Williams (private comm.), failures of Bitter magnets at M.I.T. have been largely due to insulation motion. Insulating sheets are extruded, due to axial clamping. Teflon has been particularly prone to failure due to extrusion. Insulation can also be displaced asymmetrically, due to thermal cycling, uneven axial clamping, or perhaps even Ven-

turi pressure from the coolant. The insulation displacement leads to failure due to occlusion of coolant holes. Insulations have also been subject to embrittlement in the presence of water. The failure mode may be crack growth, beginning on the inside of a sheet and moving radially outward. Williams believes this has been a particular problem with polyimide insulation. Williams suggests that failure due to insulation motion could be cured by bonded construction. Weggel, however, states that on the one occasion that bonding was used, the epoxy acted more like a lubricant than a bond. Strings of epoxy were extruded into the coolant passages and flushed into the cooling system.

Another class of magnet failures is due to gradual loosening of axial clamping and gradual increase of contact resistance. Increase in contact resistance appears to be caused by seepage of water into the contact area, followed by progressive oxidation of the contacts. The increased resistance of the magnet is detected before any gross failure occurs, and the magnet is replaced. Williams suggests that failure due to contact oxidation can be cured by gold plating contacts.

According to R. Weggel, approximately 20 magnets per year are replaced at FBNML, including magnets which have not failed, but are temporarily taken out of service and refurbished. Of those magnets which fail, roughly 50% can have the cause of failure diagnosed. Failure mechanisms include the following.

1. *Insulation shrinkage.* All insulations used at the Magnet Laboratory have been subject to some shrinkage in the presence of water. Apparently, the water diffuses into the bulk of the insulation, and under the applied compressive stress manages to combine with the insulation in such a way that shrinkage, rather than swelling, always occurs. Insulation shrinkage has been a particular problem with Kapton, and Kapton sheets in direct contact with water are no longer used. One alternative is Teflon-coated Kapton; another is the use of a resin, reinforced with both glass and Kapton. Teflon is also superior to Kapton in preventing capillary wetting of the entire insulation surface by water. High pressure, high temperature, and the presence of water drive the polymerization reaction of Kapton in the opposite direction, depolymerizing it back to a brittle monomer. Failure usually takes the form of a catastrophic magnet burnout. Shrinkage is most dramatic when

the insulation is allowed to dry. This can occur when water flow is reduced from its nominal value. Once a stack of insulation was removed in seemingly good condition from a magnet removed from service, but on drying overnight shrank dramatically.

2. *Excessive load pressure on the insulator.* Compressive load does not lead to extrusion of the insulation into coolant passages, according to Weggel, but rather leads to turn-to-turn shorts, due to insulation puncture. This can be caused by the presence of chips in the insulating sheets or localized stresses due to plate overlap at the joints.

3. *Loose sealant.* Water passages can become blocked by the escape of pipe dope or RTV from water seals.

4. *Plate corrosion.* Water can enter the joint between overlapping turns and cause local hot spots. This failure mechanism can frequently be detected before a disastrous failure occurs. When 1/2% of the central field is lost, a magnet is generally taken out of service.

5. *CuO whiskers.* Copper oxide whiskers grow in the water channels parallel to both the water flow and the electric field. After several months of operation, whiskers of 5–10 mil have been observed. When an older magnet is disassembled, a black, granular powder is observed in the vicinity of the magnet disassembly. This is assumed to be the loosely attached whiskers. These whiskers are suspects, but have not been definitively connected to any magnet failure.

A new technique using copper-clad polyimides to prevent insulation decay is being tried experimentally. Both faces of the insulating sheet are copper-clad, so that water cannot be in direct contact with either face. If the magnets are not assembled with special care, the joints can fail by a turn-to-turn short

through the cladding, when the insulation overlaps across a joint. None of the magnets using copper-clad insulation have been in service long enough to judge whether a significant improvement in reliability has been made. Failures of joints due to copper corrosion are still observed.

### 5.2.2. The ANU 30 T Electromagnet

The Australian National University electromagnet is of particular interest, because of its high performance and the care with which it was constructed and documented.<sup>(19–21)</sup> The 30 T magnet is a hybrid, consisting of an outer Bitter solenoid magnet with a self field of 16.5 T and an inner, wound magnet. The purpose of using a hybrid is to achieve most of the theoretical advantage of continuously varying magnet current density with radius without making magnet construction impractically complex. The major dimensions and performance of the two solenoids are from Carden<sup>(19)</sup> and are listed in Table VI.

The outer solenoid is a Bitter magnet, which requires 26 MW of power at 150 V and 168 kA. Cooling water is delivered to it at a rate of 6.8 kl/min at 1.7 MPa. The calculated hoop stress is highest at the inside radius, with a peak of 275 MPa (40 ksi), while the axial compressive stress builds up to 83 MPa (12 ksi) at the median plane. The conductor is hard rolled silver-copper (0.07% silver) with a nominal thickness of 0.518 mm. The insulation is 0.08 mm “Pyre ML” bonded glass fabric. The construction method is that common to all Bitter solenoids with a few innovations. In order to reduce the axial compression required for good turn-to-turn bonding, 16 discs were interwound in a staggered pattern, dispersing the slits and increasing the friction bonding. This method of construction also brings the strength of the magnet up to 15/16 that of an ideal

Table VI. The Australia National University 30 T Magnet

Parameter	Units	Inner solenoid	Outer solenoid	Total
Inside diameter	(cm)	5.62	26.75	Total
Outside diameter	(cm)	23.35	68.50	
Length	(cm)	20.30	41.40	
Field contribution	(T)	13.5	16.5	30.0
Power	(MW)	4.0	25.5	29.5
Cooling water flow	(kl min <sup>-1</sup> )	1.5	5.3	6.8
Current	(kA)	26.7	168	194.7
Voltage	(V)	150	150	

continuous plane helix. Thickness variations between disks were reduced by sorting by weight into 16 groups. Thickness variations within a disk tended to be systematic "humps," which were corrected by grinding the middle of each eighth disc of the solenoid.

The ANU design considered the possibility of failure along a helical fault path, called the unwinding mode. This failure mode would result in radial growth and twisting about the axis of the solenoid. In order to eliminate the possibility of failure through the unwinding mode, radial key bars were attached to the discs at each end of the solenoid and to appropriate slots in two stainless steel discs, welded to two locked cylinders, encasing the solenoid. The discs and cylinders form a torsion jacket, which strongly resists twisting. The inner solenoid consists of 11 concentric, nested subcoils. All of the subcoils are run electrically in parallel, so that there is no layer-to-layer voltage under normal operation. Cooling channels were identical axial grooves, 1 mm square.

The ANU inner solenoid had an interesting solution to the problem of water erosion of the interturn insulation. A number of epoxies were tested, but even the most water resistant resin allowed the diffusion of water from the exposed edge of the adhesive layer. The penetration distance was proportional to the square root of time and was approximately 1 mm in 6 months. The failure mechanism was chemical competition between the water and the epoxy to bond with the copper, resulting in replacement of epoxy by a blue compound on the copper surface. Since wetting occurred from both sides, destruction of the 2 mm wide insulation on the innermost subcoil could be expected in 6 months. The solution was to cover the bonded metal surfaces with a phenol formaldehyde baked coating, formulated especially for its high resistance to water penetration. In accelerated tests with this method, no deterioration was observed after the equivalent of 18 months exposure to water.

The parallel winding of the inner subcoils effectively eliminated the electric field between layers. In order to assure that metal and interturn insulation in different layers would align with each other, each turn was carefully spaced during bonding, using a lathe, and a helical groove was subsequently machined in the outer surface of each subcoil along the bond line. Subcoils were inspected with great care for interturn short circuits due to burrs or scratches. A several kilohertz search coil was used to find the vicinity of possible faults. A microscope was used for final visual location and removal of the faults.

### 5.2.3. *The Clarendon Magnet*

The inner magnet of the 16 T hybrid magnet at the Clarendon Laboratory in Oxford was designed and built by Carden, the designer of the ANU 30 T magnet, and was described by Hanley<sup>(42)</sup> and Hudson et al.<sup>(51)</sup> This magnet is of interest because it has a polyhelical winding. As described above, solenoids with polyhelical windings have considerably higher performance than Bitter solenoids in theory, but are sufficiently more difficult to construct that very few have been constructed. The three known examples of high performance polyhelical magnets at Clarendon, Canberra, and Grenoble are discussed here.

The Clarendon inner magnet provides 9.5 T of the total 16 T of the hybrid magnet system. The magnet current is 4750 A, the power consumption is 1.6 MW, and the peak subcoil temperature is 77 C. The polyhelical winding consists of 10 coils in six electrically serial groups. Each coil is 10 cm long with 40 turns. The radial thickness of the coils ranges from 0.2 to 1.6 cm, and the inner clear bore of the magnet is 5.0 cm. The conductors are hard-temper copper with 0.05% silver. Axial coolant channels in the original polyhelical magnet were formed by machining grooves into the outside surface of each subcoil, then tightly fitting a cylinder of glass-reinforced epoxy over each subcoil. This was the same technique used previously by Carden in the Canberra magnet.<sup>(21)</sup>

As in the Canberra magnet, the coils are terminated by pressure contacts. In the Clarendon magnet, there is an arrangement of rocking copper bridges and copper rods to transmit the hydraulic clamping force. The contacts have caused most of the operational problems of the Clarendon magnet. Shortly after installation, one of the lead pairs burnt out, presumably due to a momentary loss of contact pressure. After repair, a second lead pair burnt out. This time the cause was traced to insulation failure resulting from water absorption. The axial leads had been brought out in rings of opposite current polarity, in order to simplify the support against forces due to the fringe radial field. An inadequate epoxy insulation between lead rings of opposite polarity was permeated by water, leading to excessive leakage current. The voltage between lead rings was 400 V. After extensive insulation testing, a new lead design was implemented, using a superior wet epoxy system, designated AY111. The copper was wetted with the epoxy, followed by slipping a heat shrinkable sleeving



over the lead, followed by wetting the sleeve with epoxy (P. Hudson, Clarendon Laboratory, private comm., 1981). The establishment of reproducible contact resistance also proved to be difficult. This problem was solved by gold-plating relevant areas and by redesigning the rocker housings to assure freedom of motion. In the original design, rod motion was impeded by swelling of the glass-fiber housings after long immersion in water.

A burnout in 1981 was due to overly thick turn-to-turn insulation, leading to axial compression and loss of contact at the leads. This led to a redesign of the turn-to-turn insulation and the axial cooling channels.<sup>(53)</sup> The turn-to-turn insulation is now the dry-film adhesive, Redux 308A. This is a nylon modified epoxy with high elongation, which can be edge-wound between the turns of the helix. The epoxy flows very little on curing, allowing tight control over the glue-line. The film bonds readily to copper, requiring no prior pretreatment. The milled axial cooling channels were replaced by bonded spills. As of July, 1982, this magnet had operated for a few hundred hours without incident.

#### 5.2.4. Duplex I and II at Grenoble

The Service National des Champs Intenses is a French scientific service institute for research in the area of high field, high pressure, and low temperature. In 1972, the high field facilities were expanded to include a 10 MW power supply and 6 available magnet bays.<sup>(80)</sup> Perhaps the most interesting of the high field magnets at this site are two polyhelix resistive magnets, consisting of 12 helices, between 3.14 and 3.86 mm thick and 130 or 132 mm long, used consecutively as inserts in the 25 T hybrid magnet, called Duplex I, and renamed Duplex II when the outer Bitter magnet was upgraded from 7 T to 10 T. The resistance of each helix is fixed such that a radial constant stress current distribution is achieved.<sup>(89)</sup> The magnet is designed to generate 14.5 T with a dissipation of 4.8 MW in a volume of only 2.25 L. This power density represents a fivefold increase over that of the Bitter magnets at Grenoble. However, the heat flux is 430–540 W/cm<sup>2</sup>, typical of that with Bitter magnet design. The water velocity is 20 m/s, and the average copper temperature lies between 60 and 70 C. In an early hybrid test with an external Bitter magnet, some of the leads detached at a total field of 20.4 T, with the outer magnet contributing 7 T. The leads are connected by screws through

a connecting block. Separation and restraint of the leads is provided by insulating end rings. In the lead failure described above, glue ran during the epoxy fill. Radial fields on the leads then broke the bond, unbalanced the forces on an insulating ring and allowed enough displacement for a layer-to-layer short between two of the series leads.

The Duplex I and II polyhelix magnets at Grenoble are described by Schneider-Muntau.<sup>(90)</sup> The helices are wound from a copper strip of 7×4.4 mm, using a special winding machine which reduces the thickness to 3.9 mm during winding by cold working. The turn-to-turn insulation consists of glue filled with glass balls to fix the turn-to-turn distance at 0.2 mm. The 12 helices are connected in four series groups of three parallel windings. The three innermost windings are in parallel with a voltage of about 100 V between the third and fourth helix. An unbonded, fiber-glass epoxy crenellated insert is placed between the three series connected interlayer gaps. The final inner and outer diameters are fixed by machining, after curing. Design values of roughness, ranging from 35 to 100 μm, are introduced with a fine thread.

After refabricating the lead supports, the first polyhelical magnet ran for 400 h, usually up to a hybrid field of 24 T. Four hundred hours is two to three times longer than the life of Bitter magnets at Grenoble, operating at similar stresses (J. Schneider-Muntau, private comm.). The magnet was taken out of service in 1982, due to the persistent appearance of nonfatal turn-to-turn shorts, detected as 10–20% increases in the resistivity of the magnet at the highest fields. Shorts appeared only in layers 6–12 of the magnet. These could be burned out by discharging a capacitor bank through the coil. However, the time between appearance of these shorts decreased until further operation of the magnet became excessively tedious. The first two appearances of this condition occurred a month apart, but by the end of the magnet's service life, shorts were appearing almost every day. The postmortem on this magnet has not yet been performed. A new insert has been installed with a Silan coating on the glass balls to improve adhesion of the surrounding epoxy insulation.

#### 5.2.5. Ceramic Powder Jacketed Conductors: LAMPF and SIN

Probably the best documented approach to the design of a conductor for high irradiation tolerance is the use of mineral powder, jacketed conductors at the

LAMPF facility at Los Alamos<sup>(43, 44)</sup> and at the Schweizerisches Institut für Nuklearforschung (SIN) in Villigen.<sup>(39)</sup> While this technology has not demonstrated high performance capabilities to date, it is of interest because it has no known insulator failure mechanism, due to irradiation fluence.

According to A. Harvey (private comm.), LASL has built about 40 magnets with MgO insulation and SIN another 20. The principal application of the MgO powder technology is the same at both facilities, quadrupole magnets in accelerator target areas.<sup>(39, 44)</sup> None of the LAMPF magnets has failed because of electrical or mechanical failure in the bulk insulator. There have been failures in these magnets, but they were almost all because of inadequate interlocks, such as someone forgetting to turn on the water. As with the SIN magnets, none of the magnets at the LAMPF facility can be called "high-performance." They operate only up to 1000 A/cm<sup>2</sup> and 300 V with conductors rated at 1500 V by the manufacturer.

The LAMPF magnets are kept on all the time as dc magnets when the accelerators are up, which is about 60–70% of the time. Since most of these magnets were built in the mid-1970s, this implies service lives of greater than 30,000 h. On the basis of this experience, Harvey questioned the hypothesis that electrolysis was a real failure mechanism in MgO, under actual magnet operating conditions. The LAMPF magnets have a rather low electric field and are typically run with peak copper temperatures of less than 100 C, while Narayan's experiments on electrolysis in MgO were at elevated temperatures and fields.<sup>(75)</sup>

Harvey is not sure what the integrated radiation in the SIN magnets is, stating that dosimetry at  $> 10^9$  rads in relatively inaccessible and radioactively hot structures is difficult to achieve. One clue to the accumulated dosage is that the residual activation of the SIN magnets is  $>$  than  $10^4$  rad/h. Harvey recalled that the insulation of the neutron flux detectors in the Canadian Pickrell reactors was irradiated to  $10^{14}$  rads in the first three full power years (Reuter-Stokes Canada, Ltd., private comm., 1980). No insulation failures occurred. When the detectors were removed from service, the insulation resistance had changed from  $10^9$  to  $10^8 \Omega$  at 100 V. When a radiation detector with MgO insulation for electrical isolation burnt out after an irradiation of  $10^{14}$  rad, it was the sensing element, rather than the insulation, which failed. There have been electrical failures in MgO

powder insulation at bends and terminations, but never in the bulk insulation. Several magnets are operating with bends with minimum radii no greater than six times the flat-to-flat height of the conductor. According to Harvey, bending with great care might achieve bending radii of five times the conductor height.

According to George,<sup>(39)</sup> a total of 24 magnets had been built for the SIN accelerator facility by 1975, using solid mineral insulated cable. Indirect cooling by stainless steel pipe was chosen, in order to avoid copper and braze corrosion by the cooling water. The cable was solid copper, insulated by MgO powder in a copper sheath. The filling factor was only 30–40%. Cable ends were sealed to prevent moisture penetrating into the magnesium oxide, which is hygroscopic. The SIN magnets were designed to avoid splices, which were considered risky. Current levels were up to three times the manufacturer's recommendations. Current levels were considered to be set by the necessity for an uncooled length of about 15 cm at the cable end with a permissible temperature difference of about 100 C over this length. This allowed a cable current of 900 A versus the manufacturer's recommendation of 300 A. The current density over the cable was 1.4 kA/cm<sup>2</sup>. Thermal stresses are reduced by inserting a flexible section. The temperature of the ceramic assembly is limited only by the melting point of the braze material. By 1975, some of the quadrupole magnets had been operated successfully for over a year. Some coils were rejected on delivery; one due to internal water leakage, one due to irreparable loss of insulation resistance; in another, a water distribution block leaked at a braze. After transportation from San Francisco to Villigen, Switzerland, 10 of 192 terminations had to be replaced.

#### 5.2.6. *The Triumph Septum Magnet*

The Triumph septum magnet, used to separate a pion beam from a high intensity proton beam, was built in Canada by Gathright.<sup>(38)</sup> This magnet took an approach to radiation hardening, with potentially higher magnet performance than the mineral powder in a jacket approach described above. In this magnet, metallized Al<sub>2</sub>O<sub>3</sub> spacers were brazed to a hollow rectangular copper conductor. The spacers had dimensions of  $3/4 \times 3/4 \times 1/16$  in. The two major surfaces were molybdenum-manganese coated and held in place by brazing directly to the copper con-

ductors in a hydrogen atmosphere furnace. The conductor achieved 5000 A in a 0.4×0.8 in. conductor. Including the 1/16 in. spacers, this is 1.8 kA/cm<sup>2</sup>, which is nearly comparable in performance to an epoxy-potted hollow conductor. However, the coil is very small, consisting of only 18 turns and a terminal voltage of 13 V. Several attempts were necessary, before the coil worked. Some of the problems, such as water leaks, don't appear to be fundamental, but weakening of the copper by the repeated heat cycling required appears to be a basic drawback of this construction technique.

## 6. CONCLUSIONS

Since the development of computational techniques which allow magnets to operate to their design stress limits, progress in the performance of normal magnets has been slow. Future breakthroughs in normal magnet design will probably not be in the areas of operation at higher mechanical stresses or higher field-bore products, but in magnet reliability. The work that has been done on the stress limitations of magnets has allowed the present level of high performance to be reached, so that magnets should not fail due to bulk material stress limits. The failure mechanisms are almost entirely due to surface electrochemistry. When the failure mechanisms involve bulk material, they involve the diffusion of gases or water through the bulk material. The dominant reason that magnets have not enjoyed any systematic attacks on their causes of failures is that medium to large size air core magnets have had no commercial applications. This lack of motivation is particularly severe for normal magnets, which, while they are used extensively in support of solid-state, particle, and plasma physics experiments, did not have any imagined commercial applications, even in the distant future, until they were identified as a key component of the tandem mirror axicell plug magnet system. Although they have been proposed for tokamak bundle divertor applications<sup>(90)</sup> and compact tokamak hybrid reactors, mirror plug magnets are the only application that would provide sufficient motivation for the needed development program, since the reliability and performance of two small normal magnets has a first-order impact on the overall economics of the tandem mirror fusion reactor.

Even within the severe funding limitations of an engineering discipline with no commercial applica-

tion, the lack of focus in magnet development, insulation qualification, and material testing is not necessary. The qualification of electrical equipment by numerous IEEE and ANSI standards has been successfully accomplished for motors, generators, transformers, and circuit breakers, all of which are inherently more complex than air-core magnets. Similarly, the chemistry of magnet failures is not inherently more complex than that of problems routinely solved by chemical engineers. The problems and the solutions to the design of long-lived magnets lie at the interfaces between the conductor, the insulation, and the coolant. The accelerated life tests done by Carden on the ANU magnet turn-to-turn insulation<sup>(21)</sup> give a strong hint as to how screening for longer-lived interface systems can be accomplished at modest cost. Using scarce funds exclusively on tests of bulk mechanical properties or more sophisticated techniques for calculating mechanical stresses will not achieve the goal of long-lived, high-performance, highly irradiated magnets.

## REFERENCES

1. A. O. Allen et al., Decomposition of water and aqueous solutions under mixed fast neutron and gamma radiation, *J. Phys. Chem.*, **56**:575 (1952).
2. A. O. Allen, The yields of free H and OH in the irradiation of water, *Radiation Res.* **1**:85 (1954).
3. A. O. Allen, *J. Am. Chem. Soc.* **77**:852 (1955).
4. L. L. Alston, ed. *High-Voltage Technology* (Oxford University Press, 1968).
5. R. A. Anderson, 1974 *Annu. Rpt. CEIDP*, 435 (1975).
6. R. A. Anderson and J. P. Brainard, *J. Appl. Phys.* **51**:1414 (1980).
7. ASME Power Boiler Code, Section III, Nuclear Power Plant Components, Article XIII-1000.
8. Aymar et al., TORE SUPRA: Basic Design Tokamak System, Association Euratom-C.E.A. Report EUR-CEA-FC-1068 (Oct. 1980).
9. R. Baldi et al., Tandem demonstration facility magnet system: final report, to be published (1982).
10. C. Bazan, High field magnets, 6th Int. Conf. Mag. Tech. (MT-6), Bratislava, Czech. (Aug. 1977).
11. K. D. Bergeron and D. H. McDaniel, *Appl. Phys. Lett.* **29**:534 (1976).
12. L. Blumenau et al., TFTR TF coil support restraint structure, Proc. 8th Symp. Eng. Probs. Fusion Res., San Francisco (Oct. 1979).
13. J. Booth et al., The manufacture of the toroidal field coils of the Joint European Torus, 6th Int. Conf. Mag. Tech. (MT-6), Bratislava, Czech. (Aug. 1977).
14. A. W. Boyd, M. B. Carver, and R. S. Dixon, Computed and experimental product concentrations in the radiolysis of water, *Radiat. Phys. Chem.* **15**:177-185 (1980).
15. F. M. Bruce, Calibration of uniform field spark gaps for high-voltage measurements at power frequencies, *J. Inst. Elect. Engrs.* **100**:145 (1953).

16. J. P. Brainard and J. D. Cross, 1972 *Annu. Rpt. CEIDP*, 298 (1973).
17. L. Buff, Maintenance of coolants, in *Reactor Handbook, Vol. IV*, S. McLain and J. H. Martens, eds. (Wiley-Interscience, New York, 1964).
18. W. F. Campbell and U. B. Thomas, *Trans. Electrochem. Soc.* **91**:623 (1947).
19. P. O. Carden, Design principles relating to the strength and structure of the ANU 30 T electromagnet, *Sci. Instrum. E*, 654 (1972).
20. P. O. Carden, The design and construction of the outer solenoid of the ANU 30 T electromagnet, *Sci. Instrum. E*, 658 (1972).
21. P. O. Carden, Design and construction of the inner solenoid of the ANU 30 T electromagnet, *Sci. Instrum. E*, 663 (1972).
22. P. O. Carden, An historical review of the development of high-field electromagnets, particularly with regard to the theory of mechanical strength and the limits of performance, *Rep. Progr. Phys.* **39**:1017-1066 (1976).
23. P. A. Chatterton and D. K. Davies, *Proc. VIII-DEIV*, D2.1-11 (1978).
24. F. W. Clinad et al., Electrical insulators for the first wall of an implosion-heated theta-pinch fusion reactor, Los Alamos Sci. Lab. Rep. LA-UR-75-1687, High-Beta Pulsed Reactor Workshop, Leningrad, USSR (Sept. 1975).
25. F. W. Clinard, L. W. Hobbs, and G. F. Hurley, Neutron irradiation damage in MgO, Al<sub>2</sub>O<sub>3</sub> and MgAl<sub>2</sub>O<sub>3</sub> ceramics, Int. Conf. Neutron Irradiation Effects in Solids, Argonne, Ill., Los Alamos Report LA-UR 81-3549 (Nov. 1981).
26. R. R. Colman, Jr., and C. E. Klabunde, Mechanical strength of low temperature irradiated polyimides: a five to tenfold improvement in dose resistance over epoxies, 2nd Topical meeting on Fusion Reactor Materials, Seattle (Aug. 1981).
27. J. D. Cross, *IEEE Trans. Elec. Insul.* **EI-13**:145 (1978).
28. T. W. Dakin, The endurance of electrical insulation, Proc. 4th Symp. Elect. Insul. Materials, Japanese IEE (Sept. 1971).
29. M. V. Davis, in *Nuclear Applications of Non-Fissionable Ceramics*, A. Boltax and J. H. Handwerk, eds. (Am. Nucl. Soc., 1966), p. 229.
30. A. G. Day, in *High-Voltage Technology*, L. L. Alston, ed. (Oxford University Press, 1968).
31. L. Dorra, Bestimmung der Kupfer-Korrosionsrate in Kühlkreisläufen eines Protonenbeschleunigers, Schweizerisches Institut für Nuklearforschung Tech. Mem. TM-D1-23 (Nov. 1981).
32. E. A. Erez and Becker, Radiation damage in thin sheet fiberglass insulations, Int. Cryo. Mat. Conf., Geneva (1980).
33. E. A. Erez, "Summary of activation tests on insulators," M.I.T. internal memorandum, April 1980.
34. H. Etherington, ed. *Nuclear Engineering Handbook* (McGraw-Hill, New York, 1958).
35. D. Evans, J. T. Morgan, R. Sheldon, and G. B. Stapleton, Post-irradiation mechanical properties of epoxy resin/glass composites, Rutherford High Energy Laboratory Report RHEL/R 200 (June 1970).
36. A. Fryszman, T. Strzyz, and M. Wasinski, *Bull. Acad. Polon. Sci. Ser. Sci. Tech.* **8**:379 (1960).
37. D. I. Garber and R. R. Kinsey, Neutron cross sections: volume II, curves, Brookhaven National Laboratory Report BNL-325 (Jan. 1976).
38. T. R. Gathright and P. Reeve, A radiation hard septum magnet, *IEEE Trans. Mag.* **MAG-17**(5): (Sept. 1981).
39. D. George, Magnets with mineral insulated coils at S.I.N., 5th Int. Conf. Mag. Tech. (MT-5), Rome, (April, 1975).
40. J. Gerhold, High voltage problems at low temperatures, 7th Int. Conf. Mag. Tech., Bratislava, Czech. (Aug. 1977).
41. P. M. Gleichauf, *J. Appl. Phys.* **22**:766 (1951).
42. P. E. Hanley, IEEE Proc. Appl. Superconductivity Conf., Annapolis, N.Y. (1972), p. 302.
43. A. Harvey, Experience with the LAMPF mineral-insulated magnets, Sixth Int. Conf. Magnet Technol., Bratislava, Czech. (1977).
44. A. Harvey, High-current density coils for high-radiation environments, 7th Int. Conf. Magnet Technol., Karlsruhe, West Germany (March, 1981).
45. Haarman and Williamson, Electrical breakdown and tracking characteristics of pulsed high voltages in cryogenic helium and nitrogen, *Adv. Cryogenic Eng.* **21**: (1975).
46. J. M. Haughian et al., The design and development of multi-megawatt beam dumps, *IEEE Trans. Nucl. Sci.* **NS-24**(3): (1977).
47. W. E. Harbaugh, R. C. Buader, and W. A. Novajovsky, Final Report: Water cooled d.c. heat sink development, performed by RCA Corp for University of California, Lawrence Livermore Laboratory (Sept. 1977).
48. J. A. Horak and T. H. Blewitt, *Phys. Stat. Sol. (A)* **4**:721 (1972)
- 48(a). F. Hoyer, M. Bourges, and R. Deltenre, Radiolytic corrosion and related problems in the cooling water circuits of high energy particle accelerators, CERN 68-2 (1968).
49. F. Hoyer, Gestzmassigkeiten und Verhinderung der radiolytischen Korrosion in den Kupferleitungen der Kühlkreisläufe von Protonenbeschleunigern, *Atompraxis* **15**: Heft 2 (1969).
50. M. A. Hoffman and T. J. Duffy, Water-cooled U-tube grids for continuously operated neutral-beam injectors, Lawrence Livermore Laboratory Report UCRL-82878 (Nov. 1979).
51. P. A. Hudson, P. E. Hanley, and P. O. Carden, Exceptional aspects of high power resistive solenoids in relation to their use in hybrid magnet systems, 5th Int. Conf. Magnet Technol., Rome (April 1975).
52. G. F. Hurley and J. M. Bunch, Swelling and thermal diffusivity changes in neutron irradiated ceramics, *Am. Ceramic Soc. Bull.* **59**, No. 4 (1980).
53. P. A. Hudson and H. Jones, High field facilities and services of the Clarendon Laboratory, University of Oxford, U.K., *IEEE Trans. Mag.* **MAG-17**, No. 5 (Sept. 1981).
54. G. F. Hurley et al., Structural properties of MgO and MgAl<sub>2</sub>O<sub>4</sub> after fission neutron irradiation near room temperature, Second Topical Meeting on Fusion Reactor Materials, Seattle (Aug. 1981).
55. K. van Hulst, Engineering and cryogenic aspects of the Nijmegen 25 tesla hybrid magnet, *IEEE Trans. Mag.* **MAG-17**, No. 5 (Sept. 1981).
56. K. F. Hwang and S. O. Hong, Dielectric breakdown of liquid and vapor helium in bulk and across epoxy insulation, IEEE Proc. Applied Superconductivity Conf. (1978).
57. B. A. Johnson, Corrosion of metals in deionized water at 38 C, NASA Report No. TM X-1791 (March 1969).
58. H. G. Johnson, M. W. Liberi, and T. G. Meighan, Electrical insulation system development experiences and test results for TFTR magnetic field coils, 8th Symp. Eng. Probs. Fusion Res. San Francisco (1979).
59. Yu. K. Katrukhin, B. P. Khrustalev, and K. A. Trojnar, Glued pancake coils for Bitter solenoids, *IEEE Trans. Mag.* **MAG-17**, No. 5 (Sept. 1981).
60. K. Kawasaki et al., The toroidal field coil for JT-60, Proc. 6th Int. Conf. Magnet Technol. (MT-6), Bratislava, Czech. (Sept. 1977).
61. R. W. Klaffky et al., *Phys. Rev.* **8**, 21, 3610 (1980).
62. L. Knutsson, E. Mattsson, and B-E. Ramberg, Erosion/corrosion in copper water tubing, *Br. Corros. J.* **7**:208 (Sept. 1972).
63. A. A. Koch, J. C. Rauch, and K.-J. Greve, Insulation systems and winding technique for large coils in fusion experiments, 6th Int. Conf. Mag. Tech. (MT-77), Bratislava, Czech. (Aug. 1977).
64. Landolt and Börnstein, *7. Teil: Elektrische Eigenschaften II*

- (*Elektrochemische System*) (Springer Verlag, Berlin, 1960), p. 263.
65. J. R. Last, Poloidal coils and transformer core for JET—design and manufacture, *IEEE Trans. Mag.* **MAG-17**, No. 5 (Sept. 1981).
  66. R. V. Latham, *High Voltage Vacuum Insulation* (Academic Press, New York, 1981).
  67. M. J. Leupold et al., 30 Tesla hybrid magnet facility at the Francis Bitter National Magnet Laboratory, *IEEE Trans. Mag.* **MAG-17**, No. 5 (Sept. 1981).
  68. A. L. London, Heat transfer conditions in high power klystron tubes, Varian Associates Report 87-800-112 (Oct. 1970).
  69. G. F. Lynch, Ionic and gamma-ray induced photoconductivity of MgO *Can. J. Phys.* **53**:210 (1975).
  70. I. K. Marshakov, The corrosion of certain metals and alloys in de-ionized water, *Zashchita Metallov* **11**(1):3–9 (1975).
  71. D. May and H. Krauth, Influence of the electrode surface condition on the breakdown of liquid helium, *IEEE Trans. Mag.* **MAG-17**, No. 5 (Sept. 1981).
  72. B. McGrath et al., Mechanical tests on irradiated organic materials from BBC-Baden, CERN Rep. LAB II-RA (37, 40), TM/74-21 (1974).
  73. F. C. Moon, The virial theorem and scaling law for superconducting magnet systems, Cornell University Report (1982) (to appear in *J. Appl. Phys.*).
  74. N. F. Mott, *J. Inst. Metals* **72**:367 (1946).
  75. J. Narayan, R. A. Weeks, and E. Sonder, Aggregation of defects and thermal-electric breakdown in MgO, Oak Ridge National Laboratory Solid State Division Report 78-08 (Jan. 1978).
  76. Y. Ohki and K. Yahagi, *J. Appl. Phys.* **46**:3695 (1975).
  77. Ch. Olivier, Performance of electrodes at the first voltage breakdown in liquid helium, *IEEE Trans. Mag.* **MAG-17**, No. 5 (Sept. 1981).
  78. F. W. Peek, *Dielectric Phenomena in High-Voltage Engineering* (McGraw-Hill, New York, 1920).
  79. L. J. Perkins, Radiation dose-rate resistivity degradation in ceramic insulators and assessment of the consequences in fusion reactor applications, University of Wisconsin Report UWFD-469 (April, 1982).
  80. J. C. Picoche, P. Rub, and H.-J. Schneider-Muntau, The High Field Magnet Laboratory of Grenoble, *J. Magnetism Magnetic Mat.* **11**:308 (1979).
  81. R. Poehlchen, M. Huguet, and J. Booth, The design of the toroidal field coils for the Joint European Torus (JET), Proc. 6th Int. Conf. Magnet Technol. (MT-6), Bratislava, Czech. (Aug. 1977).
  82. M. W. Poole, Design and construction of the programmed quadrupole magnets for the Daresbury Electron Synchrotron, 5th Int. Conf. Magnet Technol. (MT-5), Rome (April, 1975).
  83. M. A. Prelas, J. B. Romero, and E. F. Pearson, A Critical Review of Fusion Systems for Radiolytic Conversion of Inorganics to Gaseous Fuels, *Nucl. Technol. Fusion* **2**(2):143 (April 1982).
  84. R. E. Renman, J. J. Sredniawski, and P. W. Trester, Results of an insulator materials test program for applications inside the TFTR plasma chamber, Proc. 9th Symp. Eng. Probs. Fus. Res., Chicago (Oct. 1981).
  85. A. H. Roebuck, C. R. Breden, and S. Greenberg, Corrosion of structural materials in high purity water, *Corrosion* **13**:71 (Jan. 1957).
  86. A. Rönquist, The oxidation of copper: a review of published data, *J. Inst. Metals*, **89**:65 (1961).
  87. J. H. Schultz, Proc. Mtg. Electrical Insulators Fusion Magnets (CONF-801237, DOE, 1981), p. 4.1.
  88. H. A. Schwarz, *J. Phys. Chem.* **66**:255 (1962).
  89. H.-J. Schneider-Muntau and P. Rub, Proc. 5th Int. Conf. Magnet Tech, Rome (1975), p. 398.
  90. H.-J. Schneider-Muntau, Polyhelix magnets, *IEEE Trans. Mag.* **MAG-17**, No. 5 (Sept. 1981).
  91. L. Simoni, A general approach to the endurance of electrical insulation under temperature and voltage, *IEE Trans. Elec. Insul.* **EI-16**, No. 4 (Aug. 1981).
  92. Von H. Sick, Die Erosionsbeständigkeit von Kupferwerkstoffen gegenüber strömendem Wasser, *Werkstoffe und Korrosion*, 23 Jahrg Heft 1 (1972).
  93. G. E. Smith, TFTR toroidal field coil design, Proc. 7th Symp. Eng. Probs. Fus. Res., Knoxville, Tenn. (1977), p. 15.
  94. T. S. Sudarshan and T. D. Cross, *IEEE Trans. Elec. Insul.* **EI-11**:32 (1976).
  95. B. Terreault et al., Further measurements of helium concentration profiles in copper and their relation to blistering, *J. Nucl. Mat.* **76/77**:249 (1978).
  96. J. Thoris, B. Leon, A. Dubois, and J. C. Bobo, Dielectric breakdown of cold gaseous helium in large gaps, *Cryogenics*, April 1970.
  97. R. Tunder, Effects of water composition on corrosion currents of copper, General Electric Report No. DF70SL119 (Dec. 1970).
  98. V. A. J. Van Lint, J. M. Bunch, and T. M. Flanagan, in *Radiation Effects and Tritium Technology for Fusion Reactors* (CONF-750989, USERDA, 1976), p. II-531.
  99. R. Weggel, High-field facilities at the Francis Bitter National Magnet Laboratory, *J. Magnetism Magnetic Mat.* **11**:321 (1979).
  100. J. Weiss, Radiochemistry of aqueous solutions, *Nature* **153**:748 (June 1944).
  101. H. J. Wintle, *Br. J. Radiol.* **33**:706.
  102. J. E. C. Williams et al., Conceptual design of a Bitter magnet toroidal field system for the ZEPHYR Ignition Test Reactor, M.I.T. Plasma Fusion Center Report PFC/RR-81-24 (May 1981).